34. Londei, M., Lamb, J.R., Bottazzo, G.F., and Feldmann, M. 1984. Epithelial cell expressing aberrant MHC class II determinants can present antigen to cloned human T cells. *Nature.* **312**:639–641.
35. Pujol-Borrell, R., et al. 1987. HLA class II induction in human islet cells by interferon-γ plus tumor necrosis factor or lymphotoxin. *Nature.* **326**:304–306.
36. Riese, R.J., et al. 1996. Essential role for cathepsin S in MHC class II-associated invariant chain processing and peptide loading. *Immunity.* **4**:357–366.
37. Buttgereit, F., Burmester, G.-R., and Brand, M.D. 2000. Bioenergetics of immune functions: fundamental and therapeutic aspects. *Immunol. Today.* **21**:192–199.
38. Balkwill, F., Foxwell, B., and Brennan, F. 2000. TNF is here to stay. *Immunol. Today.* **21**:470–471.
39. Bottazzo, G.F., Pujol-Borrell, R., Hanafusa, T., and Feldmann, M. 1983. Role of aberrant HLA-DR expression and antigen presentation in induction of endocrine autoimmunity. *Lancet.* **2**:1115–1119.
40. Fox, R.I., Bumol, R., Fantozzi, T., Bone, R., and Schreiber, R. 1986. Expression of histocompatibility antigen HLA-DR by salivary gland epithelial cells in Sjögren's syndrome. *Arthritis Rheum.* **29**:1105–1111.
41. Franco, A., et al. 1987. Class II MHC antigen expression on epithelial cells of salivary glands from patients with Sjögren's syndrome. *Clin. Exp. Rheumatol.* **5**:199–203.
42. Mircheff, A.K., et al. 1991. Class II antigen expression by lacrimal epithelial cells. An updated working hypothesis for antigen presentation by epithelial cells. *Invest. Ophthalmol. Vis. Sci.* **32**:2302–2310.
43. Germain, R.N., and Hendrix, L.R. 1991. MHC class II structure, occupancy and surface expression determined by post-endoplasmic reticulum antigen binding. *Nature.* **353**:134–139.
44. McConnell, H.M., Wada, H.G., Arimilli, S., Fok, K.S., and Nag, B. 1995. Stimulation of T cell by antigen-presenting cells is kinetically controlled by antigenic peptide binding to major histocompatibility complex class II molecules. *Proc. Natl. Acad. Sci. USA.* **92**:2750–2754.
45. Beeson, C., et al. 1996. Early biochemical signals arise from low-affinity T cell receptor-ligand reactions at the cell-cell interface. *J. Exp. Med.* **184**:777–782.
46. Rabinowitz, J.D., et al. 1997. Specific T cell recognition of kinetic isomers in the binding of peptide to class II MHC. *Proc. Natl. Acad. Sci. USA.* **94**:8702–8707.
47. Villadangos, J.A., Riese, R.J., Peters, C., Chapman, H.A., and Ploegh, H.L. 1997. Degradation of mouse invariant chain: roles of cathepsins S and D and the influence of major histocompatibility complex polymorphism. *J. Exp. Med.* **186**:549–560.
48. Deussing, J., et al. 1998. Cathepsins B and D are dispensable for major histocompatibility complex class II-mediated antigen presentation. *Proc. Natl. Acad. Sci. USA.* **95**:4516–4521.
49. Nakagawa, T., et al. 1998. Cathepsin L: critical role in Ii degradation and CD4 T cell selection in the thymus. *Science.* **280**:450–453.
50. Nakagawa, T., et al. 1999. Impaired invariant chain degradation and antigen presentation and diminished collagen-induced arthritis in cathepsin S null mice. *Immunity.* **10**:207–217.
51. Shi, G.P., et al. 1999. Cathepsin S required for normal MHC class II peptide loading and germinal center development. *Immunity.* **10**:197–206.
52. Riese, R.J., et al. 1998. Cathepsin S activity regulates antigen presentation and immunity. *J. Clin. Invest.* **101**:2351–2363.
53. Shi, G.P., et al. 2000. Role for cathepsin F in invariant chain processing and major histocompatibility complex class II peptide loading by macrophages. *J. Exp. Med.* **191**:1177–1186.

Prevention and Induction of Autoimmune Exocrinopathy Is Dependent on Pathogenic Autoantigen Cleavage in Murine Sjögren's Syndrome[1]

Kaoru Saegusa,* Naozumi Ishimaru,* Kumiko Yanagi,* Kenji Mishima,* Rieko Arakaki,* Takashi Suda,† Ichiro Saito,* and Yoshio Hayashi[2]*

The in vivo role of autoantigen cleavage during apoptosis in autoimmune diseases remains unclear. Previously, we found a cleavage product of 120-kDa α-fodrin as an important autoantigen in the pathogenesis of primary Sjögren's syndrome (SS). In the murine primary SS model, tissue-infiltrating $CD4^+$ T cells purified from the salivary glands bear a large proportion of Fas ligand, and the salivary gland duct cells constitutively possess Fas. Infiltrating $CD4^+$ T cells, but not $CD8^+$ T cells, identified significant ^{51}Cr release against mouse salivary gland cells. In vitro studies demonstrated that apoptotic mouse salivary gland cells result in a specific α-fodrin cleavage into 120 kDa and that preincubation with caspase inhibitor peptides blocked α-fodrin cleavage. In vivo treatment with caspase inhibitors *N*-benzyloxycarbonyl-Val-Ala-Asp fluoromethyl ketone and *N*-acetyl-Asp-Glu-Val-Asp-al-CHO into the murine model results in dramatic inhibitory effects on the development of autoimmune lesions and in restoration of sicca syndrome. Furthermore, we found that immunization with recombinant α-fodrin protein identical with an autoantigen into normal recipients induced autoimmune lesions similar to SS. These data indicate that prevention and induction of autoimmune exocrinopathy is dependent on autoantigen cleavage via caspase cascade and that caspase inhibitors might provide a new therapeutic option directed at reducing tissue damage in the murine model for SS. *The Journal of Immunology,* **2002, 169: 1050–1057.**

Organ-specific autoimmune diseases are characterized by tissue destruction and functional decline due to autoreactive T cells that escape self-tolerance (1, 2). Sjögren's syndrome (SS)[3] is an autoimmune disorder characterized by lymphocytic infiltrates, destruction of the salivary and lacrimal glands, and systemic production of autoantibodies to the ribonucleoprotein particles SS-A/Ro and SS-B/La (3–5). Although the specificity of CTL function has been an important issue of organ-specific autoimmune response, the mechanisms responsible for tissue destruction in SS remain to be elucidated.

We reported previously that a cleavage product of 120-kDa α-fodrin may be an important autoantigen in the pathogenesis of primary SS in both the animal model and in humans (6). α-Fodrin is a ubiquitous, calmodulin-binding protein (7) found to be cleaved by calcium-activated protease (calpain) in apoptotic T cells and by calpain and/or caspase 3 (CPP32) (8) in anti-Fas-stimulated Jurkat cells and/or neuronal apoptosis (9–12). It was demonstrated that the fodrin α subunit is cleaved in association with apoptosis and that the 120-kDa fragment is a breakdown product of the mature form of 240-kDa fodrin α subunit (11, 12). Recent reports have shown that caspase 3 is required for α-fodrin cleavage during apoptosis (12–14). In Jurkat cells, caspase 3-like proteases have been reported to cleave α-fodrin and poly(ADP-ribose) polymerase (PARP) but with differential sensitivity to the caspase 3 inhibitor *N*-acetyl-Asp-Glu-Val-Asp-al (DEVD)-CHO (14). In neuroblastoma cells, treatment with staurosporin induced cleavage of α-fodrin at both caspase 3 and calpain cleavage sites (15). Accumulating evidence indicates that the interaction of Fas with Fas ligand (FasL) regulates a large number of pathophysiological processes of apoptosis (16, 17). It has been reported that both Fas and FasL are present in thyrocytes and that their concomitant expression on thyrocytes, independent of infiltrating T cells, is responsible for thyrocyte destruction in Hashimoto's thyroiditis (18). In contrast, expression of Fas by pancreatic β cells has been shown to have a major influence on the susceptibility of tissue destruction in nonobese diabetic mice to diabetes (19, 20). Thus, we speculate that Fas-mediated cytotoxicity and caspase-mediated α-fodrin proteolysis are involved in the progression of tissue destruction in SS.

In this study, we demonstrate that an increased activity of apoptotic proteases is required for the α-fodrin proteolysis during development of murine SS. In addition, we present evidence that a cleavege product of autoantigen induces autoimmune exocrinopathy in normal recipients and that treatment with caspase inhibitors *N*-benzyloxycarbonyl-Val-Ala-Asp fluoromethyl ketone (z-VAD-fmk) and DEVD-CHO protect animals against the development of autoimmune exocrinopathy in the SS model.

Materials and Methods

Mice

Female NFS/N strain mice carrying the mutant gene *sld* (21) were reared in our specific pathogen-free mouse colony and given food and water ad

*Department of Pathology, Tokushima University School of Dentistry, Tokushima, Japan; and †Center for the Development of Molecular Target Drugs, Cancer Research Institute, Kanazawa University, Ishikawa, Japan

Received for publication December 6, 2001. Accepted for publication May 3, 2002.

The costs of publication of this article were defrayed in part by the payment of page charges. This article must therefore be hereby marked *advertisement* in accordance with 18 U.S.C. Section 1734 solely to indicate this fact.

[1] This work was supported in part by Grants-in-Aid for Scentific Research (12307040 and 12557022) from the Ministry of Education, Science and Culture of Japan. K.S. is a Research Fellow of the Japan Society for the Promotion of Science.

[2] Address correspondence and reprint requests to Dr. Yoshio Hayashi, Department of Pathology, Tokushima University School of Dentistry, 3 Kuramotocho, Tokushima 770, Japan. E-mail address: hayashi@dent.tokushima-u.ac.jp

[3] Abbreviations used in this paper: SS, Sjögren's syndrome; PARP, poly(ADP-ribose) polymerase; FasL, Fas ligand; z-VAD-fmk, *N*-benzyloxycarbonyl-Val-Ala-Asp fluoromethyl ketone; 3d-Tx, thymectomy performed on day 3 after birth; non-Tx, nonthymectomied; MSG, mouse salivary gland; FLIM, FasL inhibitory mAb; DEVD, *N*-acetyl-Asp-Glu-Val-Asp-al.

0022-1767/02/$02.00

libitum. Thymectomy was performed on day 3 after birth (3d-Tx) in NFS/*sld* mice (22). A total of 156 mice, consisting of 74 3d-Tx and 82 non-thymectomied (non-Tx) NFS/*sld* mice, were investigated in the present study. C57BL/6 mice ($n = 24$) purchased from Charles River Japan (Atsugi, Japan) were used as controls.

Histology and immunohistology

All organs were removed from the mice, fixed with 4% phosphate-buffered formaldehyde (pH 7.2), and prepared for histologic examination. The sections were stained with H&E. Histological grading of the inflammatory lesions was done according to the method proposed by White and Casarett (23). Immunohistology was performed on freshly frozen sections (4 μm in thickness) by the biotin-avidin immunoperoxidase method using avidin-biotin immunoperoxidase complex reagent (Vector Laboratories, Burlingame, CA). The mAbs used are as follows: biotinylated rat mAbs to CD3 (Life Technologies, Grand Island, NY), B220, CD4, CD8, Mac-1 (BD Biosciences, San Jose, CA), murine Fas (*clone 13*; Transduction Laboratories, Lexington, KY), and murine FasL (*K-10*; BD PharMingen, San Diego, CA).

TUNEL

Apoptotic cells were detected in sections using the in situ TUNEL kit (Wako Pure Chemical, Osaka, Japan). Briefly, sections were incubated with proteinase K (20 μg/ml) for 10 min and then presoaked in TdT buffer (0.5 mmol/L cacodylate, 1 mmol/L CoCl, 0.5 mmol/L DTT, 0.05% BSA, 0.15 mol/L NaCl) for 10 min. Sections were incubated for 2 h at 37°C in 25 μl of TdT solution containing 1× terminal transferase buffer, 0.5 nmol of biotin-dUTP, and 10 U of TdT (Wako Pure Chemical). After the TdT reaction, sections were soaked in TdT blocking buffer (300 nmol/L NaCl, 30 nmol/L tri-sodium citrate-2-hydrate), incubated with HRP-conjugated streptavidin for 30 min at room temparature, and developed for 10 min in phosphate-buffered citrate (pH 5.8) containing 0.6 mg/ml diaminobenzidine. Nuclei were counterstained with hematoxylin.

Flow cytometric analysis

Surface markers were identified by mAbs with an EPICS flow cytometer (Beckman Coulter, Miami, FL). Rat mAbs to CD3 (Life Technologies), B220, CD4, CD8 (BD Biosciences), murine Fas (*Jo2*, BD PharMingen), and murine FasL (BD PharMingen) were used. Double-labeled surface phenotypes such as CD3/B220, CD4/FasL, and CD8/FasL were analyzed. FasL expressions were analyzed on tissue-infiltrating lymphocytes in 3d-Tx NFS/*sld* mice gated on CD4 and CD8. Apoptotic cells were detected with an EPICS flow cytometer (Beckman Coulter) using the Annexin V^{FITC} Apoptosis Detection Kit (Genzyme, Cambridge, MA). For detection of T cell activation makers, single cell suspensions were stained with Abs conjugated to PE (anti-CD3, Life Technologies; anti-CD4, Cedarlane Laboratories, Hornby, Ontario, Canada; B220, BD PharMingen) and FITC (anti-CD8, Cedarlane Laboratories; Thy1.2, anti-CD44, anti-CD45RB, anti-Mel-14, BD PharMingen) and were analyzed with an EPICS flow cytometer (Beckman Coulter).

RT-PCR

Total RNA was extracted from homogenized tissues with TRIzol reagent (Life Technologies), and cDNA was prepared from RNA with 50 pmol oligo (dT) 18 and 200 U of murine leukemia virus reverse transcriptase (Life Technologies). Two microliters of the cDNA mixture was used in a PCR with 10 pmol of forward and reverse primers and 2.5 U of *Taq* DNA polymerase (PerkinElmer/Cetus, Norwalk, CT). The sequences of the specific sense and anti-sense oligonucleotide primer pairs were as follows: Fas, 5′-ATCCGAGCTCTGAGGAGGCGGGGTTCATGAAAC-3′ and 5′-GGAGGTTCTAGATTCAGGGTCATCCTG-3′; β-actin, 5′-ATGGATGACGATATCGCT-3′ and 5′-ATGAGGTAGTCTGTCAGGT-3′. Samples were amplified through 30 cycles at an annealing temperature of 58°C in a PCR Thermal Cycler (PerkinElmer/Cetus). PCR products were blotted onto nylon membrane and hybridized with ^{32}P-labeled cDNA probes.

Isolation of tissue-infiltrating cells from salivary glands

We isolated tissue-infiltrating mononuclear cells from affected salivary glands, as described previously (24, 25). In brief, affected submandibular glands from five mice were removed, cut into small pieces with scissors, passed through a 100-gauge stainless steel mesh, and suspended in RPMI 1640 containing 10% FCS, 10 mM HEPES buffer, penicillin (100 U/ml), and streptomycin (100 μg/ml). After washing twice with medium, infiltrating cells were isolated from parenchymal cells by Ficoll-Isopaque density-gradient centrifugation. $CD4^+$ and $CD8^+$ T cells were purified from infiltrating cells using magnetic beads (Dynal Biotech, Oslo, Norway).

Primary culture of mouse salivary gland (MSG) cells

Primary cultures of MSG cells were prepared as reported previously (26). Briefly, the salivary gland cells were isolated from NFS/*sld* mice at 3–5 wk by enzymatic digestion with 0.76 mg/ml EDTA and mixture of collagenase (type I, 750 U/ml) and hyaluronidase (type IV, 500 U/ml), plated in 24-well plates, and maintained in MEM containing 10% FCS for 5–7 days before flow cytometric analysis and cytotoxic assay. Apoptosis was induced in MSG cells by anti-Fas Ab (Jo2, 300 ng ml^{-1}; BD PharMingen). On Western blotting, cytosolic extracts were prepared from MSG cells (1×10^7 cells), which were treated at 37°C with apoptotic stimuli for various times.

Western blot analysis

Western blot analysis with mouse mAb to α-fodrin (Affiniti, Mamhead, U.K.) and PARP (Transduction Laboratories) were performed. Briefly, the cells were homogenated in 20 mM Tris-HCl buffer (pH 7.4) containing 5 mM diisopropylfluorophosphate, 5 mM EDTA, 5 mM benzamidine, 2 mM PMSF, and 2 mM *N*-ethylmaleimide. After centrifugation for 20 min at 12,000 rpm at 4°C, supernatant was extracted and used for cytoplasmic protein. Pellets were homogenized in 20 mM Tris-HCl buffer containing 2% Triton X-100. Protein binding was visualized with ECL Western blotting reagent (Amersham, Arlington Heights, IL). Protease inhibitors included mixtures (Sigma-Aldrich, St. Louis, MO), leupeptin (Wako Pure

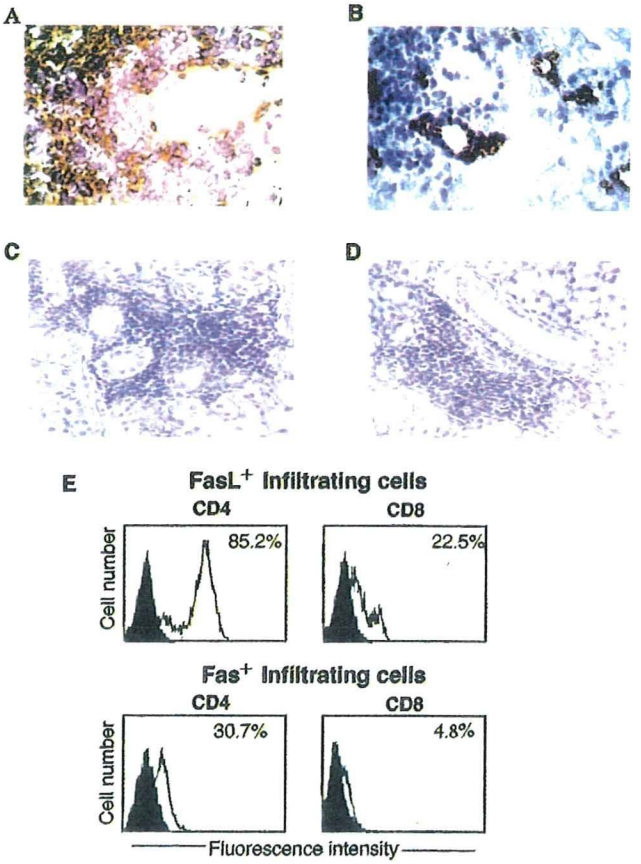

FIGURE 1. FasL and Fas expression on tissue-infiltrating cells in the salivary gland tissues from 3d-Tx NFS/*sld* mice. *A*, Immunohistochemical detection of infiltrating lymphocytes strongly positive for FasL in 3d-Tx NFS/*sld* mice. *B*, Epithelial duct cells were stained positively with Fas in 3d-Tx NFS/*sld* mice. Isotype-matched control for FasL (*C*) and Fas (*D*) were stained negatively. *E*, Flow cytometric analysis of FasL and Fas expression on tissue-infiltrating lymphocytes isolated from salivary glands of 3d-Tx NFS/*sld* mice gated on CD4 and CD8. FasL expression on tissue-infiltrating $CD4^+$ T cells was prominent compared with that on $CD8^+$ T cells. A minor proportion of infiltrating $CD4^+$ T cells express Fas, and $CD8^+$ T cells bearing Fas were negligible. Five mice in each group were analyzed at 8 and 12 wk of age, and the mean percentages were statistically significant at $p < 0.01$ (Student's t test).

Chemical), E64 (Wako Pure Chemical), and caspase inhibitors (z-VAD-fmk and Ac-DEVD-CHO; ICN Pharmaceuticals, Costa Mesa, CA). Control for protein loading was provided by actin, tubulin, and myosin. To detect serum autoantibodies against 120-kDa α-fodrin Ag (6), mouse IgG was isolated from serum samples collected from 3d-Tx NFS/*sld* mice. Samples were solubilized by heating and separated by 10% SDS-PAGE. The autoantigen was electrotransferred to nitrocellulose and then quenched with 1% powdered milk in borate-buffered saline. Nitrocellulose membranes were incubated with testing serum at a 1/200 dilution in borate-buffered saline and then incubated with peroxidase-conjugated horse anti-mouse IgG (Vector Laboratories) at a 1/1000 dilution.

Cytotoxic assay

MSG cells (2×10^6) in 7.5 ml of MEM, supplemented with 5% FBS, were labeled overnight at 37°C in 5% CO_2 with 300 μCi of sodium ^{51}Cr-chromate. $CD4^+$ and $CD8^+$ T cells isolated from salivary gland tissues and spleen ($2–3 \times 10^6$) in 0.2 ml of RPMI 1640 were supplemented with 10% FBS. Each well of 96-well microtiter plates received, in a total volume of 200 μl, target cells, effector cells in the indicated ratios, and either medium. Microplates were centrifuged for 1 min at 1500 rpm and incubated for 4 h at 37°C. After another centrifugation, 100-μl aliquots of the supernatants were assayed for radioactivity. The fraction of the total radioactivity released was then calculated, and the results, averaged from triplicates, were expressed as percent specific ^{51}Cr release (percent experimental ^{51}Cr release minus percent ^{51}Cr release from target cells alone). To examine the role of FasL for cytotoxic activities, anti-murine FasL inhibitory mAb (FLIM58) (27) was used. FLIM58 neutralizes mouse but not human FasL activity (27).

Sequential activation of caspase 1-like and caspase 3-like proteases

The caspase 1 (IL-1-converting enzyme)- and caspase 3 (CPP32)-like activity in anti-Fas Ab treated with MSG cell extracts was determined using fluorescent substrate (28). Cell lysates were diluted with 0.5 ml of IL-1-converting enzyme standard buffer and incubated at 30°C for 30 min with 1 μM fluorescent substrate. The caspase inhibitors z-VAD-fmk or Ac-DEVD-CHO were added to the reaction mixture at a concentration of 1 μM. Specific caspase 1- and caspase 3-like activities were determined by subtracting the values obtained in the presence of inhibitors. The fluorescent substrates, MOCAc-YVAD(dnp)-NH_2 and MOCAc-DEVD(dnp)-NH_2 were custom-synthesized at the Peptide Institute (Osaka, Japan). The fluorescence of the cleaved substrates

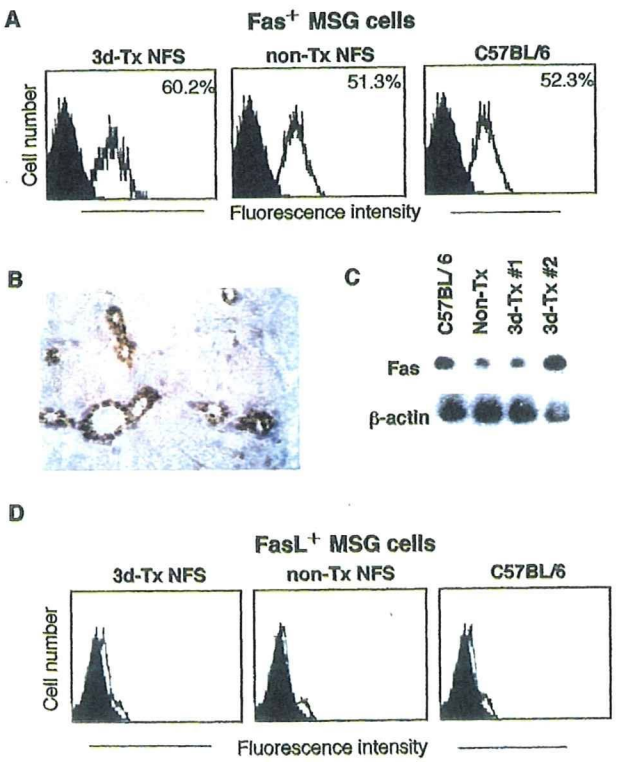

FIGURE 2. Fas expression on primary cultured MSG cells. *A*, Flow cytometric analysis of Fas expression on MSG cells from 3d-Tx, non-Tx NFS/*sld*, and normal C57BL/6 mice. Fas expression was constitutively observed on MSG cells from each group of mice. *B*, Epithelial duct cells in the salivary glands were constitutively stained with Fas in normal C57BL/6 mice. *C*, RT-PCR analysis in salivary gland tissues. Fas mRNA expression was present in C57BL/6, non-Tx NFS/*sld* mice, and 3d-Tx NFS/*sld* from two different mice. *D*, Flow cytometric analysis of FasL expression on MSG cells from 3d-Tx, non-Tx NFS/*sld*, and normal C57BL/6 mice. No significant positive cells were observed. Five mice in each group were analyzed.

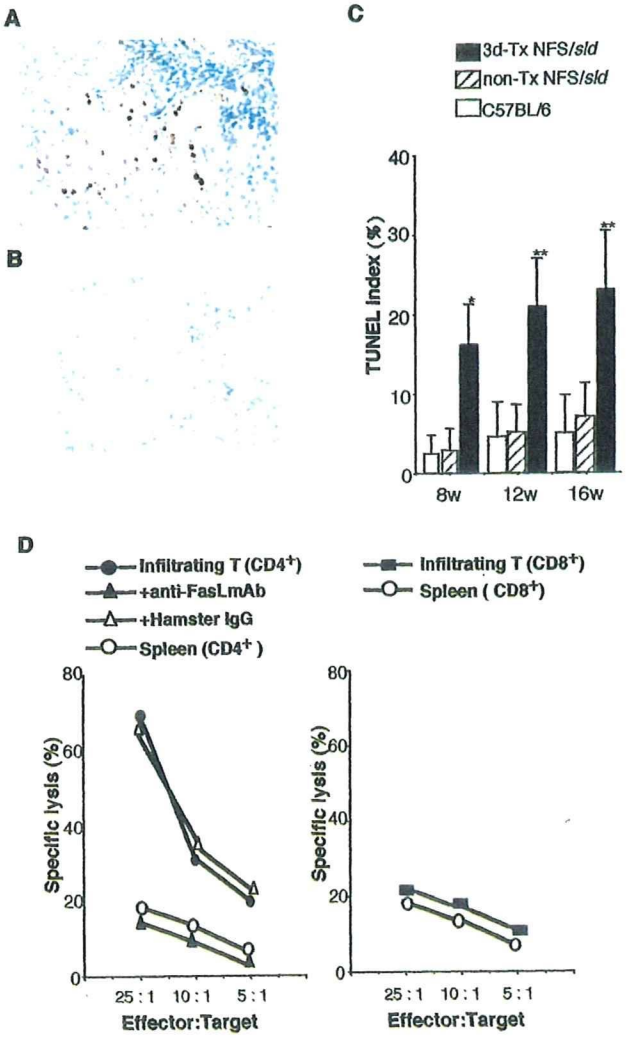

FIGURE 3. In situ TUNEL detection was frequently positive for epithelial duct cells in 3d-Tx NFS/*sld* mice (12 wk old) (*A*), but not in non-Tx NFS/*sld* mice (12 wk old) (*B*). *C*, A significant increase of apoptotic duct cells was observed in the salivary gland tissues from 3d-Tx NFS/*sld* mice at all ages. The percentage of duct cells staining positively with TUNEL was enumurated using a 10×20 grid net micrometer disc covering an objective of area 0.16 mm^2. Data were analyzed in 10 fields per section and were expressed as mean percentage $\pm$ SD in five mice examined per group. (*, $p < 0.01$; **, $p < 0.001$; Student's t test). Five mice in each group were analyzed at 8, 12, and 16 wk of age. *D*, Detection of cytotoxic activity in tissue-infiltrating $CD4^+$ T cells toward MSG cells. These activities were almost entirely inhibited by anti-murine neutralizing FasL mAb (FLIM48, 1 μg/ml). No significant cytotoxic activities were found in tissue-infiltrating $CD8^+$ T cells or in splenic $CD4^+$ and $CD8^+$ T cells toward MSG cells. The results, averaged from triplicates, were expressed as a percentage of specific ^{51}Cr release.

was determined using a spectrofluorometer set at an excitation wavelength of 328 nm and an emission wavelength of 393 nm.

In vivo administration of caspase inhibitors

To examine the therapeutic effects of i.v. injection of caspase inhibitors, a 1 mg/ml (50 μg/head) z-VAD-fmk (n = 11) and Ac-DEVD-CHO (n = 9) in DMSO were injected i.v. three times per week into 3d-Tx NFS/*sld* mice from 4 to 7 wk, because autoimmune lesions in the salivary and lacrimal glands start to develop at 3 wk of age. Dose of caspase inhibitor was determined according to the previous report (29). Mice were examined histopathologically at 8 wk and compared with 3d-Tx NFS/*sld* mice injected with DMSO alone (n = 6). In addition, autoantibody production against the 120-kDa α-fodrin in serum was tested in both treated and nontreated mice. Detection of tear and saliva volume of the treated mice and control SS animal model of 3d-Tx NFS/*sld* mice was done according to a modified method as described (26).

In vivo immunization with autoantigen

Recombinant α-fodrin protein identical with a 120-kDa cleavage product (JS-1, 5 μg/ml) (6) emulsified with CFA (Difco, Detroit, MI) was administerred twice s.c. into syngeneic normal NFS/*sld* mice at 4 and 6 wk (n = 12). At 4 and 8 wk after the s.c. injection, mice were examined on histopathological and immunological analysis. For controls, mice injected with rat brain α-fodrin (5 μl/ml; n = 10), recombinant α-fodrin protein encoding full-length α-fodrin (JS-1, 1–1784 bp; 2.7A, 2258–4884 bp; 3'DA, 3963–7083 bp; a mixture of 5 μg/ml) (n = 10) (6), lysozyme (5 μg/ml; n = 10), GST emulsified with CFA (50 μl/head; n = 10), and CFA alone (50 μl/head; n = 10) were examined. Rat brain α-fodrin was purified according to the method described previously (30).

Proliferative T cell responses

Single cell suspensions of spleen cells from treated and control mice were cultured in 96-well flat-bottom microtiter plates (5×10^5 cells/well) in RPMI 1640 containing 10% FCS, penicillin/streptomycin, and 2-ME. Cells were cultured with recombinant α-fodrin (JS-1, 5 μg/ml), rat brain α-fodrin (5 μg/ml), lysozyme (5 μg/ml, Sigma-Aldrich), and OVA (5 μg/ml, Sigma-Aldrich). During the last 8 h of the 72-h culture period, 1 μCi of [^{3}H]thymidine was added per well, and the incorporated radioactivity was determined using an automated beta liquid scintillation counter.

ELISA

Serum autoantibodies were detected using recombinant α-fodrin (JS-1). After coating with the recombinant α-fodrin in 96-well ELISA plates, biotinylated anti-mouse IgG (Vector Laboratories) was added as a second Ab. Measurements of specific autoantibodies were read by automatic ELISA reader (Flow Laboratories, McLean, VA) at 492 nm.

Results

Involvement of apoptotic cascade in tissue destruction

Histological and immunohistological characteristics of autoimmune exocrinopathy in 3d-Tx NFS/*sld* SS model mice were described in detail (22, 31, 32). To determine the possible involvement of the apoptotic cascade in tissue destruction, we examined apoptotic cells in the salivary gland specimens from 3d-Tx and non-Tx NFS/*sld* mice. Immunohistology revealed that the majority of tissue-infiltrating lymphoid cells in the salivary glands bear

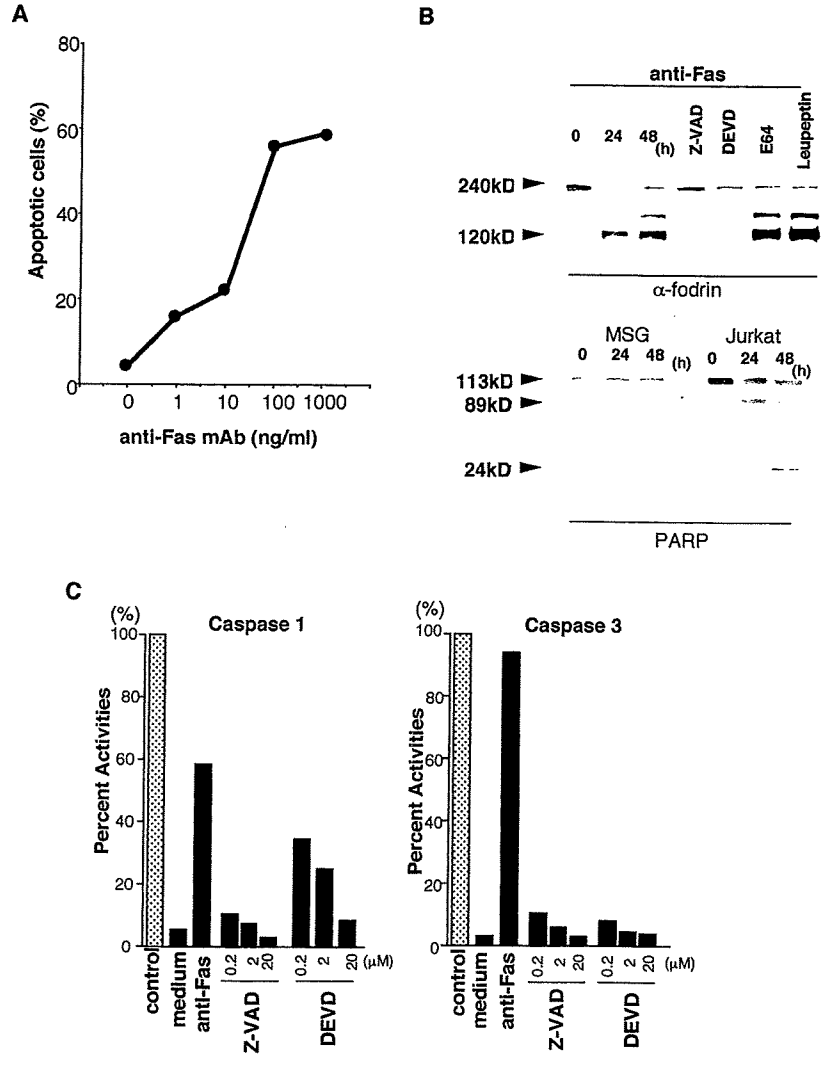

FIGURE 4. *A*, The MSG cell apoptosis induced by anti-Fas mAb (*Jo2*) stimulation determined by flow cytometry of DNA content of nuclei with propidium iodide and annexin V. *B*, Western blot analysis demonstrated that the 240-kDa α-fodrin in apoptotic MSG cells was cleaved into smaller fragments of 120 kDa in a time-dependent manner, and the cleavage product was entirely blocked by preincubation with caspase inhibitors (z-VAD-fmk and DEVD-CHO) measured at 24 h. The PARP cleavage in apoptotic MSG cells was not detected. Cleavage products of PARP (89 or 24 kDa) were detected in apoptotic Jurkat cells. Protease inhibitor mixtures, cysteine protease inhibitors (E64), and serine protease inhibitor (leupeptin) had no significant effect on α-fodrin cleavage. *C*, Activation of caspase 1-like and caspase 3-like proteases was detected during anti-Fas-induced apoptosis, and caspase inhibitors inhibited these activities at different doses (0.2, 2, and 20 μM). Cytosolic extracts were prepared from MSG cells (1×10^7 cells), which were treated at 37°C with 300 ng ml^{-1} of *Jo-2*. The 100% activity as control was calculated using the values 300 U/ml recombinant caspase 1 or caspase 3 added to each substrate (200 μM MOCAc-YVAD(dnp)-NH_2 and MOCAc-DEVD(dnp)-NH_2).

FasL in the SS model (Fig. 1*A*) and that epithelial duct cells express Fas Ag on their cell surface (Fig. 1*B*). We found that tissue-infiltrating $CD4^+$ T cells isolated from the affected glands bear a large proportion of FasL (>85%), compared with $CD8^+$ T cells bearing FasL on flow cytometry (<23%; $p < 0.01$; Fig. 1*E*). A minor proportion of infiltrating $CD4^+$ T cells express Fas (<31%), and $CD8^+$ T cells bearing Fas were negligible (<5%). Primarily cultured MSG cells isolated from 3d-Tx, non-Tx NFS/*sld* and C57BL/6 mice constitutively express Fas with high proportion (51–60%) on flow cytometry (Fig. 2*A*). Immunohistochemically, epithelial duct cells in non-Tx NFS/*sld* and C57BL/6 salivary glands are positive for Fas (Fig. 2*B*). RT-PCR analysis demonstrated that Fas mRNA was constitutively present in the salivary glands of the SS model, non-Tx NFS/*sld*, and normal C57BL/6 mice (Fig. 2*C*). MSG cells isolated from these mice did not express FasL on flow cytometric analysis (Fig. 2*D*). A significant increase of $TUNEL^+$-apoptotic epithelial duct cells in the salivary glands was observed in SS model mice, compared with those in non-Tx NFS/*sld* and C57BL/6 mice at all ages (Fig. 3, *A–C*). We next investigated whether tissue-infiltrating T cells are responsible for tissue destruction as judged by in vitro ^{51}Cr release cytotoxic assay against MSG cells. Infiltrating $CD4^+$ T cells, but not $CD8^+$ T cells, identified significant ^{51}Cr release against MSG cells (Fig. 3*D*). These cytotoxic activities were almost entirely inhibited by incubation with anti-murine neutralizing FasL mAb (FLIM58, 1 μg/ml) (Fig. 3*D*). No significant cytotoxicities were found in splenic $CD4^+$ and $CD8^+$ T cells toward MSG cells.

In vitro cleavage of α-fodrin by apoptotic proteases

We examined the in vitro cleavage of α-fodrin in MSG cells induced by anti-Fas mAb (*Jo2*, 300 ng ml^{-1}). Anti-Fas mAb-stimulated apoptosis in MSG cells was confirmed by flow cytometry of DNA content of nuclei with propidium iodide and annexin V (Fig. 4*A*). Western blot analysis demonstrated that the 240-kDa α-fodrin in apoptotic MSG cells was cleaved to smaller fragments into 120 kDa in a time-dependent manner, and the cleavage was entirely blocked by preincubation with caspase inhibitors (z-VAD-fmk and DEVD-CHO) (Fig. 4*B*). Protease inhibitor mixtures, cysteine protease inhibitors (E64), and serine protease inhibitor (leupeptin) had no significant effect on 120-kDa α-fodrin cleavage in apoptotic MSG cells (Fig. 4*B*). The 113-kDa PARP in apoptotic MSG cells was

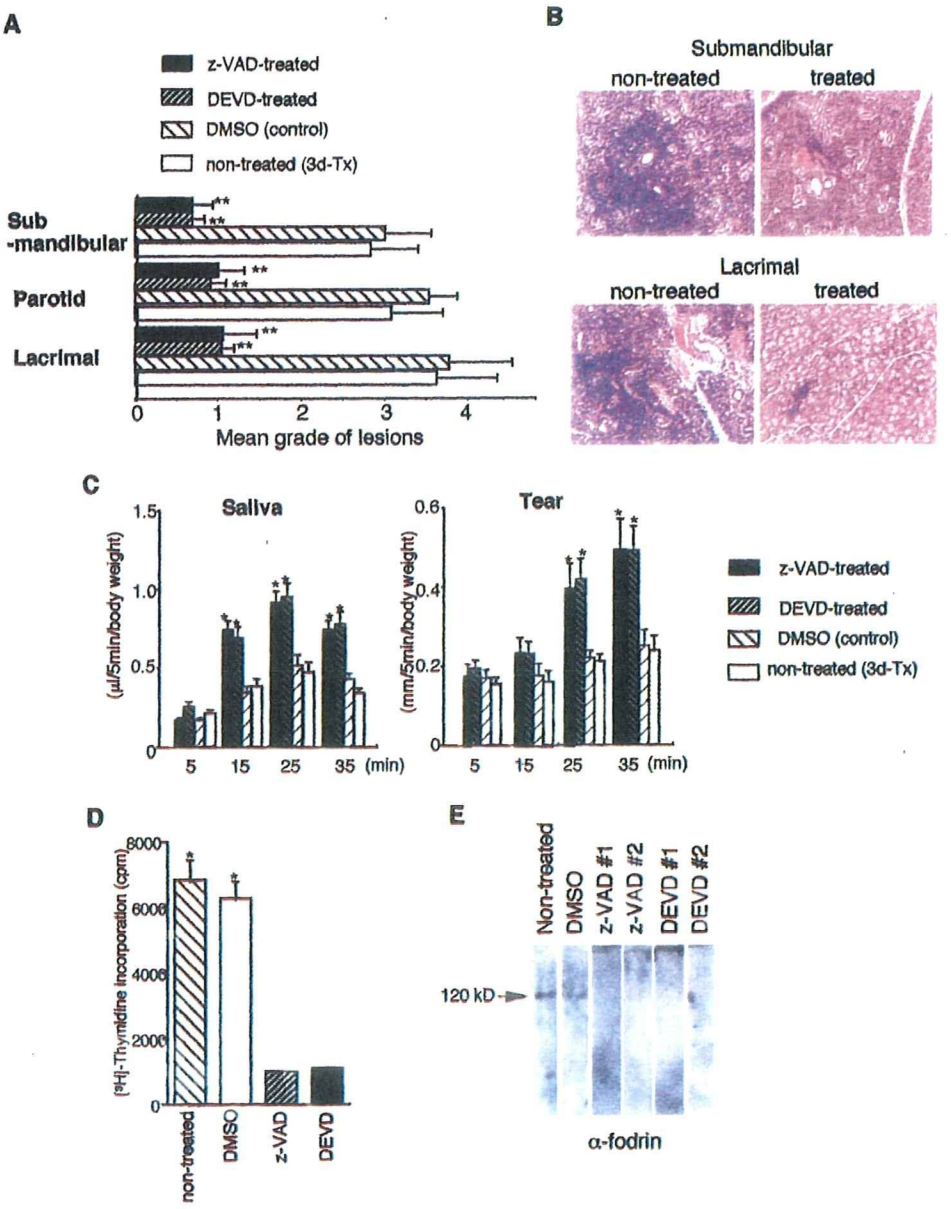

FIGURE 5. Preventive effect of i.v. injection of caspase inhibitors. One milligram per milliliter (50 μg/head) z-VAD-fmk ($n = 11$) and DEVD-CHO ($n = 9$) in DMSO was injected i.v. three times per week into 3d-Tx NFS/*sld* mice for 4–7 wk. *A*, Mice were examined histopathologically at 8 wk and compared with 3d-Tx NFS/*sld* mice injected with DMSO alone ($n = 7$) (*, $p < 0.01$; **, $p < 0.005$; Student's *t* test). *B*, Representative histologic features in the salivary and lacrimal glands showing preventive effects in z-VAD-fmk-treated mice at 8 wk of age. *C*, The average saliva and tear volume of the SS model mice treated with caspase inhibitors was significantly higher than that of control mice. Results are expressed as mean ± SEM in five mice examined per group (*, $p < 0.05$; **, $p < 0.005$; Student's *t* test). *D*, Mice treated with caspase inhibitors showed a significant decrease of autoantigen-specific T cell proliferation in spleen cells, compared with those in controls (*, $p < 0.01$; Student's *t* test). Data are expressed as cpm per culture in triplicate. *E*, Serum autoantibody production to 120-kDa α-fodrin was inhibited in sera from two different mice treated with both caspase inhibitors.

not cleaved to smaller fragments. We next investigated whether cysteine proteases are involved in α-fodrin cleavage on apoptotic MSG cells. The caspase 1- and caspase 3-like activities in anti-Fas mAb-stimulated MSG cell extracts were determined using fluorescent substrates, and caspase inhibitors (z-VAD-fmk and DEVD-CHO) inhibited these activities at different doses (0.2, 2, and 20 μM) (Fig. 4*C*).

Preventive effect of caspase inhibitors in vivo

We investigated whether the i.v. injection of caspase inhibitors protects animals against the development of autoimmune lesions. Treatment with i.v. injection of both z-VAD-fmk and DEVD-CHO (three times per week) ($p < 0.005$) prevented the development of autoimmune lesions in the salivary and lacrimal glands (Fig. 5, *A* and *B*). The average saliva and tear volume of the treated SS animal model was significantly higher than that of the control group (Fig. 5*C*). A significant decrease of autoantigen-specific T cell proliferation was observed in spleen cells from treated mice (Fig. 5*D*). In addition, serum autoantibody production against 120-kDa α-fodrin was clearly inhibited by the treatment with caspase inhibitors (Fig. 5*E*).

Induction of autoimmune lesions by immunization with autoantigen

To examine the autoimmune nature of 120-kDa α-fodrin, recombinant α-fodrin protein identical with an autoantigen was administerred s.c. into normal NFS/*sld* mice at 4 wk. Organ-specific autoimmune lesions similar to SS developed at 8 wk after the injection in almost all mice immunized with autoantigen, but not in all groups of control (Fig. 6*A*; Table I). No inflammatory lesions were observed in other organs. A majority of infiltrating cells were $CD4^+$ and $FasL^+$, and the epithelial duct cells express Fas on their cell surface (Fig. 6*A*). A minor proportion of $CD8^+$ and Fas^+ infiltrating cells was observed (data not shown). A specific cleavage of α-fodrin into 120 kDa was detected in the salivary glands of immunized mice, but not in controls (Fig. 6*B*). The activation

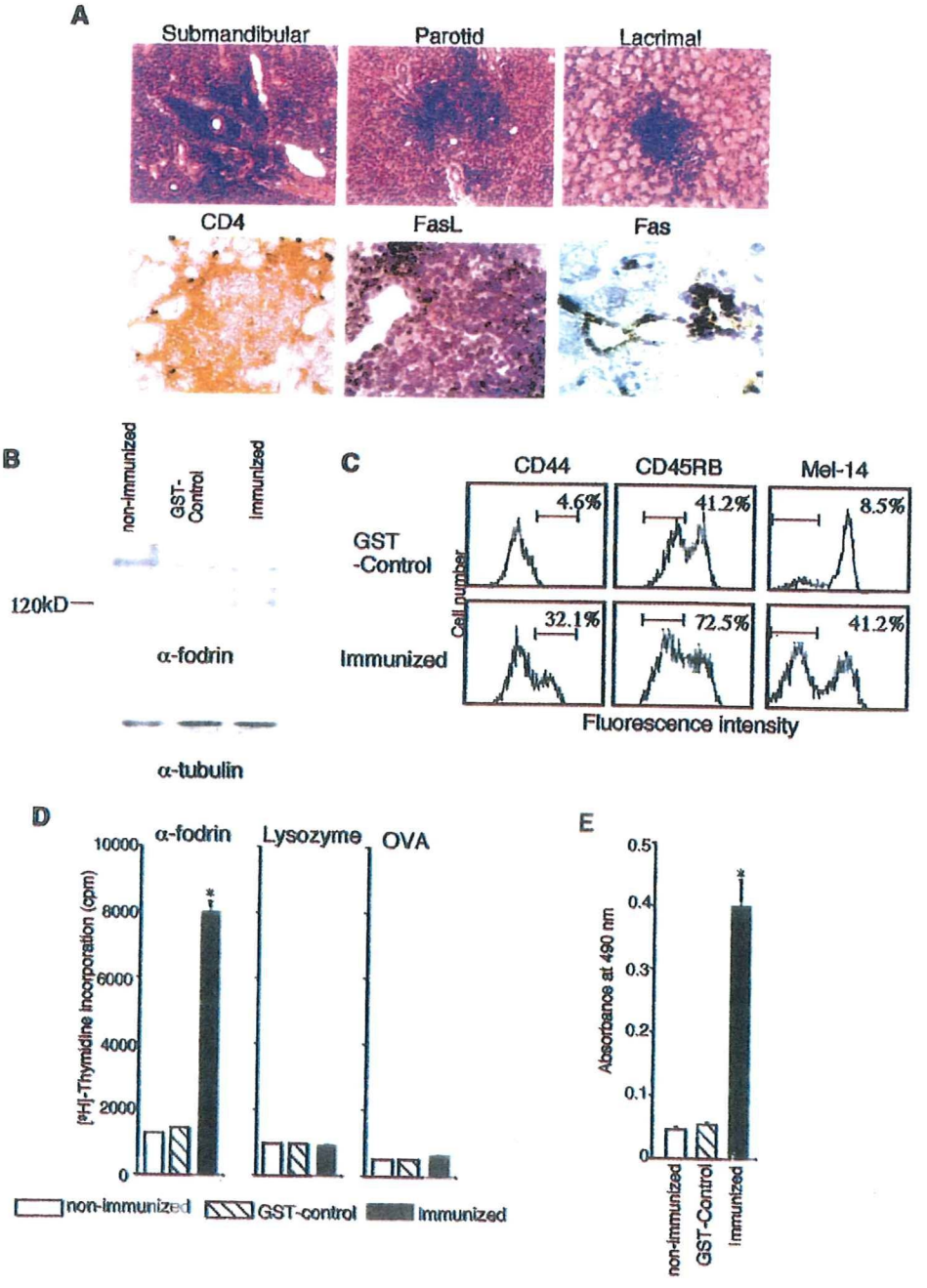

FIGURE 6. Autoimmune lesions in the salivary and lacrimal glands developing at 8 wk after the s.c. injection of autoantigen in almost all syngeneic normal mice. Representative histologic features showed in the salivary and lacrimal glands (*A*, *upper panels*, HE). A majority of infiltrating mononuclear cells were $CD4^+$ and $FasL^+$, and the epithelial duct cells express Fas on their cell surface (*A*, *lower panels*). *B*, A specific cleavage product of 120-kDa α-fodrin was detected in the salivary glands from immunized mice on Western blotting, but not in control. *C*, The activation markers ($CD44^{high}$, $CD45RB^{low}$, and $Mel\text{-}14^{low}$) were up-regulated in spleen cells gated on CD4 from immunized mice, compared with control mice. *D*, Mice injected with α-fodrin autoantigen showed a significant increase of autoantigen-specific T cell proliferation in spleen cells, whereas no responses were observed against lysozyme and OVA (*, $p < 0.05$; Student's *t* test). Data are expressed as cpm per culture in triplicate. *E*, A higher titer of serum autoantibodies against 120-kDa α-fodrin was detected by ELISA in immunized mice compared with that of control mice (*, $p < 0.05$; Student's *t* test).

Table I. *Frequency of inflammatory infiltrates in autoimmune exocrinopathy of autoantigen-administered normal NFS/*sld *mice*

Weeks After Last Immunization	No. of Mice	No. of Mice with Lesions[a]		
		Submandibular	Parotid	Lacrimal
4 wk				
Immunized[b]	6	2/6	2/6	1/6
Brain fodrin[c]	5	0/5	0/5	0/5
Full-length α-fodrin[c]	5	0/5	0/5	0/5
Lysozyme[c]	5	0/5	0/5	0/5
GST[c]	5	0/5	0/5	0/5
CFA alone[d]	5	0/5	0/5	0/5
8 wk				
Immunized	6	6/6	6/6	5/6
Brain fodrin	5	0/5	0/5	0/5
Full-length α-fodrin	5	0/5	0/5	0/5
Lysozyme	5	0/5	0/5	0/5
GST	5	0/5	0/5	0/5
CFA alone	5	0/5	0/5	0/5

[a] Histological evaluation of the inflammatory lesions was done according to the method proposed by White and Casarett (23).

[b] Syngeneic normal NFS/*sld* mice were immunized with recombinant α-fodrin autoantigen (5 μg/ml) (6) emulsified with CFA twice s.c. at 4 and 6 wk (n = 12). At 4 and 8 wk after the s.c. injection. the immunized mice were analyzed.

[c] Normal NFS/*sld* mice were injected with rat brain α-fodrin, full-length α-fodrin, lysozyme, and GST-emulsified CFA twice s.c. at 4 and 6 wk and were analyzed at 4 and 8 wk after the injection (n = 10 for each).

[d] Normal NFS/*sld* mice were injected with CFA alone (50 μl/head) twice s.c. at 4 and 6 wk and were analyzed at 4 and 8 wk after the injection (n = 10).

markers ($CD44^{high}$, $CD45RB^{low}$, $Mel\text{-}14^{low}$) were up-regulated in spleen cells gated on CD4 from immunized mice, compared with controls (Fig. 6*C*). Mice injected with recombinant autoantigen showed a significant increase of autoantigen-specific T cell proliferation in spleen cells (Fig. 6*D*). A high titer of serum autoantibodies against 120-kDa α-fodrin was detected in immunized mice, compared with control mice, by ELISA (Fig. 6*E*). These data strongly suggest that a cleavage product of 120-kDa α-fodrin is a pathogenic autoantigen on the development of murine primary SS.

Discussion

Cleavage of certain autoantigens during apoptosis may reveal immunocryptic epitopes that could potentially induce autoimmune responses in systemic autoimmune diseases (33, 34). Among the substrates cleaved during apoptosis are nuclear autoantigens targeted in systemic autoimmune diseases such as PARP (35, 36), U1–70-kDa (37), the nuclear lamin (38, 39), and DNA-dependent kinase (40). However, the in vivo role of autoantigen cleavage during apoptosis in autoimmune diseases remains unclear.

We reported previously that a cleavage product of 120-kDa α-fodrin may be an important autoantigen in the development of primary SS, and anti-120-kDa α-fodrin Abs have been frequently detected in sera from patients (6). Because it was shown that the fodrin α subunit is cleaved in association with apoptosis and the 120-kDa fragment is a breakdown product of the mature form of 240-kDa fodrin α subunit (11, 12), we examined the in vitro cleavage of α-fodrin using primarily cultured MSG cells. We clearly detected 120-kDa α-fodrin in anti-Fas-induced apoptotic MSG cells by Western blotting. We found that a significant increase of $TUNEL^+$-apoptotic epithelial duct cells in the salivary glands was detected in the 3d-Tx NFS/*sld* SS model compared with those in non-Tx NFS/*sld* mice at all ages. MSG cells constitutively express Fas with high proportion, and tissue-infiltrating $CD4^+$ T cells isolated from the salivary gland tissues of the SS model mice bear a large proportion of FasL. Moreover, we confirmed that tissue-infiltrating $CD4^+$ T cells, but not $CD8^+$ T cells, are responsible for tissue destruction as judged by in vitro ^{51}Cr release cytotoxic assay against MSG cells in vitro. These cytotoxic activities were inhibited by incubation with anti-murine neutralizing FasL mAb. Although it has been reported that Fas-induced apoptosis seems to be the major killing pathway of the $CD4^+$ cytotoxic T cells (41), our data suggest that one mechanism by which activated $CD4^+$ T cells induce cytotoxicity toward salivary gland cells in the murine SS model is Fas based. When we investigated whether cysteine proteases are involved in α-fodrin cleavage, the caspase 1- and caspase 3-like activities in anti-Fas Ab-treated MSG cell extracts were determined using fluorescent substrates. In apoptotic MSG cells, caspase inhibitors (z-VAD-fmk and DEVD-CHO) inhibited the formation of 120-kDa α-fodrin, whereas protease inhibitor mixtures, other cysteine protease inhibitors (E64), and serine protease inhibitor (leupeptin) had no effect on 120-kDa α-fodrin cleavage in apoptotic MSG cells. Furthermore, the treatment of the murine SS model with i.v. injection of z-VAD-fmk and DEVD-CHO prevented the development of autoimmune conditions, resulting in restoration of saliva and tear secretion. These results suggest that increased activity of the caspase cascade is involved in the progression of α-fodrin proteolysis during the initial stages of the development of primary SS. Moreover, we obtained experimental evidence that immunization with recombinant α-fodrin protein identical with an autoantigen is sufficient to induce autoimmune SS lesions in normal recipients, but not with rat brain α-fodrin or with recombinant full-length α-fodrin. These results indicate that caspase-mediated α-fodrin cleavage into the 120-kDa fragment plays a critical role in the development of autoimmmune exocrinopathy in primary SS and suggest that the primary mediators of the disease are autoantigen-driven T cell responses.

When human T cell leukemia CEM cells were induced to undergo apoptosis, the 240-kDa α-fodrin was cleaved to a single detectable fragment of 120 kDa (42). It is plausible that the 120-kDa fragment is a breakdown product of the 150-kDa α-fodrin cleavage (9). There is increasing evidence that the cascade of caspases is a critical component of the cell death pathway (43–45), and a few proteins have been found to be cleaved during apoptosis. These include PARP, a small U1 nuclear ribonucleoprotein, and α-fodrin, which were subsequently identified as substrates for caspases (35–37). We provided evidence that α-fodrin is cleaved by one or more members of caspases during apoptotic cell death in SS salivary glands. Fodrin cleavage by caspases can potentially lead to cytoskeletal rearrangement, and it is of interest to point out that α-fodrin binds to ankylin, which contains a cell death domain (46). In contrast, it has been shown that cleavage products of α-fodrin inhibit ATP-dependent glutamate and γ-aminobutyric acid accumulation into synaptic vesicles (47), supposing that a cleavage product of 120-kDa α-fodrin could be a novel component of an unknown immunoregulatory network such as cytolinker proteins (48).

Taken together, these results are strongly suggestive of essential roles of caspase cascade for α-fodrin cleavage leading to tissue destruction in autoimmune exocrinopathy of primary SS. Moreover, in vivo preventive effects against autoimmune lesions treated with caspase inhibitor have important implications for testing useful therapies.

References

1. Gianani, R., and N. Satventnick. 1989. Virus, cytokine, antigens, and autoimmunity. *Proc. Natl. Acad. Sci. USA 93:2252.*
2. Feldmann, M., F. M. Bennan, and R. N. Maini. 1996. Rheumatoid arthritis. *Cell 85:307.*
3. Fox, R. I., C. A. Robinson., J. G. Curd, F. Kozin, and F. V. Howell. 1986. Sjögren's syndrome: proposed criteria for classification. *Arthritis Rheum. 29:577.*

4. Chan, E. K., J. C. Hamel, J. P. Buyon, and E. T. Tan. 1991. Molecular definition and sequence motifs of the 52-kD component of human SS-A/Ro autoantigen. *J. Clin. Invest, 87:68.*
5. Kruize, A. A., R. J. T. Smeenk, and L. Kater. 1995. Diagnostic criteria and immunopathogenesis of Sjögren's syndrome: implications for therapy. *Immunol. Today 16:557.*
6. Haneji, N., T. Nakamura, K. Takio, K. Yanagi, H. Higashiyama, I. Saito, S. Noji, H. Sugino, and Y. Hayashi. 1997. Identification of α-fodrin as a candidate autoantigen in primary Sjögren's syndrome. *Science 276:604.*
7. Leto, T. L., S. Pleasic, B. G. Forget, E. J. Benz, Jr., and V. T. Marchesi. 1989. Characterization of the calmodulin-binding site of nonerythroid α-spectrin. *J. Biol. Chem. 264:5826.*
8. Alnemri, E. S., D. J. Livingstin, D. W. Nicholson, G. Salvensen, N. A. Thornberry, W. W. Wong, and J. Yuan. 1996. Human ICE/CED-3 protease nomenclature. *Cell 87:171.*
9. Martin, S. D., G. A. O'Brien, W. K. Nishioka, A. J. McGahon, A. Mahboubi, T. C. Saido, and D. R. Green. 1995. Proteolysis of fodrin (non-erythroid spectrin) during apoptosis. *J. Biol. Chem. 270:6425.*
10. Martin, S. D., D. M. Finucane, G. P. Amarante-Mendes, G. A. O'Brien, and D. R. Green. 1996. Phosphatidylserine externalization during CD95-induced apoptosis of cells and cytoplasts requires ICE/CED-3 protease activity. *J. Biol. Chem. 271:28753.*
11. Vanags, D. M., I. Pörn-Ares, S. Coppolaa, D. H. Burgess, and S. Orrenius. 1996. Protease involvement in fodrin cleavage and phosphatidylserin explosure in apoptosis. *J. Biol. Chem. 271:31075.*
12. Nath, R., K. J. Raser, D. Stafford, I. Hajimohammadreza, A. Posner, H. Allen, R. V. Talanian, P.-W. Yuen, R. B. Gilbertsen, and K. W. Wang. 1996. Nonerythroid α-spectrin breakdown by calpain and interleukin 1β-converting-enzyme-like protease(s) in apoptotic cells: contributory roles of both protease families in neuronal apoptosis. *Biochem. J. 319:683.*
13. Janicke, R. U., M. L. Sprengart, and A. G. Porter. 1996. Caspase-3 is required for α-fodrin cleavage but dispensable for cleavage of other death substrates in apoptosis. *J. Biol. Chem. 273:15540.*
14. Cryns, V. L., L. Bergeron, H. Zhu, H. Li, and J. Yuan. 1996. Specific cleavage of α-fodrin during Fas- and tumor necrosis factor-induced apoptosis is mediated by an interleukin-1β-converting enzyme/Ced-3 protease distinct from the poly-(ADP-ribose) polymerase protease. *J. Biol. Chem. 271:31277.*
15. Wang, K. W., R. Posmantur, R. Nath, K. McGinnis, M. Whitton, R. V. Talanian, S. B. Glantz, and J. S. Morrow. 1998. Simultaneous degradation of αII- and βII-spectrin by caspase 3 (CPP32) in apoptotic cells. *J. Biol. Chem. 273:22490.*
16. Nagata, S., and T. Suda. 1995. Fas and Fas ligand: *lpr* and *gld* mutations. *Immunol. Today 16:39.*
17. Maria, R. D., and R. Testi. 1998. Fas-FasL interactions: a common pathogenic mechanism in organ-specific autoimmunity. *Immunol. Today 19:121.*
18. Giordano, C., G. Stassi, R. De Maria, M. Todaro, P. Richiusa, G. Papoff, G. Ruberti, M. Bagnasco, R. Testi, and R. Galluzzo. 1997. Potential involvement of Fas and its ligand in the pathogenesis of Hashimoto's thyroiditis. *Science 275:960.*
19. Chervonsky, A. V., Y. Wang, F. S. Wong, I. Visintin, R. A. Flavell, C. A. Janeway, Jr., and L. A. Matis. 1997. The role of Fas in autoimmune diabetes. *Cell 89:17.*
20. Itoh, N., A. Imagawa, T. Hanahusa, M. Waguri, K. Yamamoto, H. Iwahashi, M. Moriwaki, H. Nakajima, J. Miyagawa, M. Namba, et al. 1997. Requirement of Fas for the development of autoimmune diabetes in nonobese diabetic mice. *J. Exp. Med. 186:613.*
21. Hayashi, Y., A. Kojima, M. Hata, and K. Hirokawa. 1988. A new mutation involving the sublingual gland in NFS/N mice: partially arrested mucous cell differentiation. *Am. J. Pathol. 132:187.*
22. Haneji, N., H. Hamano, K. Yanagi, and Y. Hayashi. 1994. A new animal model for primary Sjögren's syndrome in NFS/*sld* mutant mice. *J. Immunol. 153:2769.*
23. White, S. C., and G. W. Casarett. 1974. Induction of experimental autoallergic sialadenitis. *J. Immunol. 112:178.*
24. Hayashi, Y., N. Haneji, H. Hamano, and K. Yanagi. 1994. Transfer of Sjögren's syndrome-like autoimmune lesions into SCID mice and prevention of lesions by anti-CD4 and anti-T cell receptor antibody treatment. *Eur. J. Immunol. 24:2826.*
25. Ishimaru, N., K. Saegusa, K. Yanagi, N. Haneji, I. Saito, and Y. Hayashi. 1999. Estrogen deficiency accelerates autoimmune exocrinopathy in murine Sjögren's syndrome through Fas mediated apoptosis. *Am. J. Pathol. 155:173.*
26. Saito, I., K. Haruta, M. Shimuta, H. Inoue, H. Sakurai, K. Yamada, N. Ishimaru, H. Higashiyama, T. Sumida, H. Ishida, et al. 1999. Fas ligand-mediated exocrinopathy resembling Sjögren's syndrome in mice transgenic for IL-10. *J. Immunol. 162:2488.*
27. Miwa, K., H. Hashimoto, T. Yatomi, N. Nakamura, S. Nagata, and T. Suda. 1999. Therapeutic effect of an anti-Fas ligand mAb on lethal graft-versus-host disease. *Int. Immunol. 11:925.*
28. Enari, M., R. V. Talanian, W. W. Wong, and S. Nagata. 1996. Sequential activation of ICE-like and CPP32-like proteases during Fas-mediated apoptosis. *Nature 380:723.*
29. Rodriguez, I., K. Matsuura, C. Ody, S. Nagata, and P. Vassalli. 1996. Systemic injection of a tripeptide inhibits the intracellular activation of CPP32-like proteases in vivo and fully protects mice against Fas-mediated fulminant liver destruction and death. *J. Exp. Med. 184:2067.*
30. Cheney, R., J. Levin, and M. Willard. 1986. Purification of fodrin from mammalian brain. *Methods Enzymol. 134:42.*
31. Takahashi, M., Y. Mimura, H. Hamano, N. Haneji, K. Yanagi, and Y. Hayashi. 1996. Mechanism of the development of autoimmune dacryoadenitis in the mouse model for primary Sjögren's syndrome. *Cell. Immunol. 170:54.*
32. Hayashi, Y., N. Haneji, H. Hamano, K. Yanagi, M. Takahashi, and N. Ishimaru. 1996. Effector mechanism of experimental autoimmune sialadenitis in the mouse model for primary Sjögren's syndrome. *Cell. Immunol. 171:217.*
33. Utz, P. J., M. Hottelet, P. H. Schur, and P. Anderson. 1997. Proteins phosphorylated during stress-induced apoptosis are common targets for autoantibody production in patients with systemic lupus erythematosus. *J. Exp. Med. 185:843.*
34. Casiano, C. A. 1996. Selective cleavage of nuclear autoantigens during CD95 (Fas/APO-1)-mediated T cell apoptosis. *J. Exp. Med. 184:765.*
35. Tewan, M., L. T. Quan, K. O'Rouker, S. Desnoyers, Z. Zeng, D. R. Beidler, G. G. Poirier, G. S. Salvesen, and V. M. Dixit. 1995. Yama/CPP32β, a mammalian homolog of CED-3, is a CrmA-inhibitable protease that cleaves the death substrate poly(ADP-ribose) polymerase. *Cell 81:801.*
36. Nicholson, D. W., A. Ali, N. A. Thornberry, J. P. Vaillancourt, C. K. Ding, M. Gallant, Y. Gareau, P. R. Griffin, M. Labelle, Y. A. Lazebnik, et al. 1995. Identification and inhibition of the ICE/CED-3 protease necessary for mammalian apoptosis. *Nature 376:37.*
37. Casciola-Rosen, L., D. W. Nicholson, T. Chong, K. R. Rowan, N. A. Thornberry, D. K. Miller, and A. Rosen. 1996. Apopain/CPP32 cleaves proteins that are essential for cellular repair: a fundamental principle of apoptotic death *J. Exp. Med. 183:1957.*
38. Oberhammer, F. A., K. Hochegger, G. Froschl, R. Tiefenbacher, and M. Pavelka. 1994. Chromatin condensation during apoptosis is accompanied by degradation of lamin A+B, without enhanced activation of cdc2 kinase. *J. Cell Biol. 126:827.*
39. Neamati, N., A. Fernandez, S. Wright, J. Kiefer, and D. J. McConkey. 1995. Degradation of lamin B1 precedes oligonucleosomal DNA fragmentation in apoptotic thymocytes and isolated thymocyte nuclei. *J. Immunol. 154:3788.*
40. Casciola-Rosen, L. A., G. J. Anhalt, and A. Rosen. 1995. DNA-dependent protein kinase is one of a subset of autoantigens specifically cleaved early during apoptosis. *J. Exp. Med. 182:1625.*
41. Hahn, S., R. Gehri, and P. Erb. 1995. Mechanism and biological significance of CD4-mediated cytotoxicity. *Immunol. Rev. 146:57.*
42. Patel, T., G. J. Gores, and S. H. Kaufmann. 1996. The role of proteases during apoptosis. *FASEB J. 10:587.*
43. Holtzman, D. M., and M. Deshmukh. 1997. Caspases: a treatment target for neurodegenerative disease? *Nat. Med. 3:954.*
44. Rudel, T., and G. M. Bokoch. 1997. Membrane and morphological changes in apoptotic cells regulated by caspase-mediated activation of PAK2. *Science 276: 1571.*
45. Huang, S., Y. Jiang, Z. Li, E. Nishida, P. Mathias, S. Lin, R. J. Ulevitch, G. R. Nemerow, and J. Han. 1997. Apoptosis signaling pathway in T cells is composed of ICE/Ced-3 family proteases and MAP kinase kinase 6β. *Immunity 6:739.*
46. Feinstein, E., A. Kimchi, D. Wallach, M. Boldin, and E. Varfolomeev. 1995. The death domain: a module shared by proteins with diverse cellular function. *Trends Biochem. Sci. 20:342.*
47. Ozkan, E. D., F. S. Lee, and T. Ueda. 1997. A protein factor that inhibits ATP-dependent glutamate and γ-aminobutyric acid accumulation into synaptic vesicles: purification and initial characterization. *Proc. Natl. Acad. Sci. USA 94:4137.*
48. Brown, M. J., J. A. Hallam, K. M. Yamada, and S. Shaw. 2001. Integration of human T lymphocyte cytoskeleton by cytolinker protein. *J. Immunol. 167:641.*

ARTHRITIS & RHEUMATISM
Vol. 46, No. 6, June 2002, pp 1585–1594
DOI 10.1002/art.10315

Suppression of Tumor Necrosis Factor α–Induced Matrix Metalloproteinase 9 Production in Human Salivary Gland Acinar Cells by Cepharanthine Occurs via Down-Regulation of Nuclear Factor κB

A Possible Therapeutic Agent for Preventing the Destruction of the Acinar Structure in the Salivary Glands of Sjögren's Syndrome Patients

Masayuki Azuma, Keiko Aota, Tetsuya Tamatani, Katsumi Motegi, Tsuyoshi Yamashita, Yuki Ashida, Yoshio Hayashi, and Mitsunobu Sato

Objective. **Our previous results suggested that suppression of tumor necrosis factor α (TNFα)–induced matrix metalloproteinase 9 (MMP-9) could prevent the destruction of acinar tissue in the salivary glands of patients with Sjögren's syndrome (SS). The present study was undertaken to investigate the effect of cepharanthine on the suppression of TNFα-induced MMP-9 production in NS-SV-AC, an SV40-immortalized normal human acinar cell clone.**

Methods. **After pretreatment with or without cepharanthine, NS-SV-AC cells were treated with TNFα alone or with a combination of TNFα and cepharanthine. The expression of MMP-9 was then examined at the protein and messenger RNA levels. In addition, the effect of cepharanthine on the morphogenetic behavior of NS-SV-AC cells cultured on type IV collagen–coated dishes in the presence of TNFα was examined.**

Results. **Although TNFα induced the production of MMP-9 in NS-SV-AC cells, this production was greatly suppressed when cells were pretreated with cepharanthine, followed by treatment with both TNFα and cepharanthine. In addition, cepharanthine suppressed the TNFα-stimulated NF-κB activity by partly preventing the degradation of IκBα protein in NS-SV-AC cells. When NS-SV-AC cells were seeded on type IV collagen–coated dishes in the presence of both TNFα and plasmin, type IV collagen interaction with the cells was lost and the cells entered apoptosis. However, pretreatment with cepharanthine restored the aberrant in vitro morphogenesis of the NS-SV-AC cells.**

Conclusion. **These results may indicate a molecular mechanism by which cepharanthine is able to protect against the destruction of the acinar structure in salivary glands from patients with SS.**

Sjögren's syndrome (SS), one of the most common rheumatic diseases (1), is characterized by the eventual total replacement of the acinar structure by marked infiltration of lymphocytes into the salivary and lacrimal glands (2). The pathogenesis of this selective and progressive destruction of the acinar structure in salivary glands is not yet fully understood. However, accumulated evidence indicates a close relationship between cytokine expression in salivary gland tissue and the development and progression of this disease (3,4). Expression of messenger RNA (mRNA) for various cytokines, such as tumor necrosis factor α (TNFα), interleukin-1β (IL-1β), IL-2, and interferon-γ (IFNγ), has been detected in the salivary glands of humans as well as experimental animals during the development of SS.

Supported by grants-in-aid from the Ministry of Education, Science, Sports, and Culture of Japan.

Masayuki Azuma, DDS, PhD, Keiko Aota, DDS, PhD, Tetsuya Tamatani, DDS, PhD, Katsumi Motegi, DDS, PhD, Tsuyoshi Yamashita, DDS, Yuki Ashida, DDS, Yoshio Hayashi, DDS, MD, Mitsunobu Sato, DDS, PhD: Tokushima University School of Dentistry, Tokushima, Japan.

Address correspondence and reprint requests to Masayuki Azuma, DDS, PhD, Department of Oral and Maxillofacial Surgery 2, Tokushima University School of Dentistry, 3 Kuramoto-cho, Tokushima 770-8504, Japan. E-mail: azumasa@dent.tokushima-u.ac.jp.

Submitted for publication September 27, 2001; accepted in revised form February 7, 2002.

Establishment of the normal acinar structure of the salivary glands is fully dependent on the integrity of extracellular matrices, including the basement membrane (5). The basement membrane consists mainly of type IV collagen and laminin, and its synthesis and degradation are tightly regulated by proteolytic enzymes and their inhibitors. However, disruption of acinar cell–basement membrane interactions by excessive production of proteolytic enzymes, such as matrix metalloproteinases (MMPs), could lead to the disruption of the acinar tissue. Because cytokines, including TNFα and IL-1β, have been shown to stimulate the production of collagenases (6,7), it is conceivable that the cytokines contribute to the destruction of the basement membrane, which in turn, leads to the disruption of the acinar structure of the salivary gland. Moreover, structural changes in the basement membrane of salivary glands and increased levels of latent and active MMP-9 in saliva have recently been demonstrated in SS patients (8,9). Taken together, these observations support the previous finding that MMP-9 is implicated in the pathogenesis of SS (10).

The type IV collagenase MMP-9 is an important determinant of the degradation of the basement membrane (11). The promoter region of the MMP-9 gene has been found to contain binding sites for nuclear factor κB (NF-κB) (12), and production of MMP-9 has been reported to be stimulated by TNFα (13). NF-κB, one of the major components induced by TNFα, is considered to be an important transcription factor in the regulation of the MMP-9 gene. Under nonstimulated conditions, NF-κB is retained in the cytoplasm by its inhibitory protein, IκBα. The binding of IκBα to NF-κB masks nuclear localization signals in NF-κB and prevents its translocation to the nucleus (14). Conversely, upon stimulation by external stimuli, such as TNFα, IκBα undergoes phosphorylation and is subsequently degraded through the ubiquitin/proteasome pathway. Degradation of IκBα leads to the nuclear translocation of NF-κB, which then stimulates the expression of its target genes (15).

Recently, we demonstrated that although NS-SV-AC cells (an SV40-immortalized normal human acinar cell clone) produced a large amount of MMP-9 in response to TNFα, a super-repressor form of IκBα (srIκBα) complementary DNA (cDNA)–transfected NS-SV-AC clone lost its responsiveness to TNFα in terms of MMP-9 production (16). In addition, suppression of TNFα-induced MMP-9 production restored the normal in vitro morphogenesis of acinar cells even when they were cultured on type IV collagen–coated plates in the presence of both TNFα and plasmin. Moreover, an immunohistochemical study using salivary gland tissue from SS patients indicated that acinar cells adjacent to the lymphocytic infiltrate exhibited enhanced expression of both MMP-9 and NF-κB compared with those distant from infiltrated lymphocytes as well as those in normal salivary glands (16,17). It therefore seems likely that inhibition of TNFα-induced MMP-9 production in acinar cells may lead to the restored integrity of the acinar structure in SS salivary glands.

Based on these considerations, we postulated a working hypothesis concerning clinical therapy for patients with SS. We thought that the identification of drugs that suppress the TNFα-induced production of MMP-9 would be a promising strategy.

Cepharanthine, a bisbenzylisoquinoline (biscoclaurine) alkaloid extracted from *Stephania cephalantha Hayata*, has been used widely for the treatment of patients with leukopenia (18), nasal allergy (19), and venomous snake bites (20). Although the exact mechanism has not been elucidated, cepharanthine exerts immunomodulatory effects by enhancing the cytotoxic effect of natural killer cells and macrophages (21,22), suggesting that it plays a possible role in the regulation of signaling pathways of cytokines.

In the present study, we examined the effect of cepharanthine on the TNFα-induced MMP-9 production in NS-SV-AC cells. We found that TNFα-induced MMP-9 production was effectively suppressed by cepharanthine through the down-regulation of NF-κB activity.

MATERIALS AND METHODS

Cells and media. The characteristics of NS-SV-AC cells have been described in detail elsewhere (23). This cell clone was cultured at 37°C in serum-free keratinocyte medium (Gibco BRL, Grand Island, NY) in an incubator with an atmosphere containing 5% CO_2.

Growth assay. Cells (1×10^4/well) were grown in 96-well plates (Falcon, Oxnard, CA) in serum-free keratinocyte medium in the presence of cepharanthine (Kaken Syouyaku, Tokyo, Japan) at concentrations of 0, 5, 10, and 20 μg/ml. After the appropriate incubation periods, 10 μl of a 5-mg/ml preparation of MTT was added to each well and incubation was continued for 4 hours. The absorbance was measured with a Titertek spectrophotometer (Flow, Irvine, UK) at 570 nm with a reference wavelength of 630 nm. All assays were run in triplicate.

Enzyme-linked immunosorbent assay (ELISA) for TNFα. For quantitative determination of TNFα produced by cepharanthine-treated NS-SV-AC cells, a microtiter-based sandwich ELISA was used. A commercially available TNFα assay kit was purchased from Genzyme Diagnostics (Cambridge, MA). Briefly, NS-SV-AC cells were treated with 10

μg/ml of cepharanthine for 4 days, and conditioned medium was concentrated by the method previously described (24). Biotinylated anti-human TNFα antibody and 100 μg of total protein from conditioned medium were added to each well of a microtiter plate coated with monoclonal anti-human TNFα antibody. Plates were then incubated for 1 hour at 37°C.

After 5 washes, 100 μl of working substrate consisting of tetramethylbenzidine and hydrogen peroxide was added, and the plates were incubated for another 10 minutes at room temperature. Optimal absorbance was then read at 450 nm using a Titertek spectrophotometer. All assays were performed in triplicate.

Substrate gel analysis. NS-SV-AC cells were pretreated for 24 hours with or without cepharanthine (10 μg/ml) and then treated for 24 hours with either TNFα (10 ng/ml) or a combination of TNFα (10 ng/ml) and cepharanthine (10 μg/ml). MMP-9 activity was assayed according to the method described previously (25). Aliquots of conditioned medium (20 μg) were mixed with sample buffer without β-mercaptoethanol, applied directly to 10% sodium dodecyl sulfate (SDS)–polyacrylamide gel containing 1 mg/ml of gelatin (Wako, Osaka, Japan), and electrophoresed.

After removal of SDS from the gel by incubation in 2.5% Triton X-100 for 30 minutes, the gel was incubated at 37°C for 14 hours in reaction buffer consisting of 50 m*M* Tris HCl, pH 7.6, 0.2*M* NaCl, 5 m*M* $CaCl_2$, and 0.02% Brij-35. MMP-9 activity was identified by its ability to clear the substrate at its characteristic molecular weight, and was visualized after staining with Coomassie blue R250.

Preparation of nuclear and cytosolic extracts. Cells were seeded on 100-mm plastic petri dishes (Falcon). Twenty-four hours after seeding, cells were pretreated with or without cepharanthine (10 μg/ml) for 24 hours, and nuclear extracts were obtained after treatment with either TNFα (10 ng/ml) alone or a combination of TNFα and cepharanthine according to previously described methods (26,27). Cells were washed twice with ice-cold phosphate buffered saline, resuspended for 15 minutes in 400 μl of ice-cold lysis buffer, consisting of 10 m*M* HEPES, pH 7.9, 10 m*M* KCl, 0.1 m*M* EDTA, 0.1 m*M* EGTA, 0.5 m*M* dithiothreitol (DTT), 0.5 mg/ml benzamidine, and 2 mg/ml aprotinin. Nonidet P-40 was added to achieve a final concentration of 0.3%, and the lysates were vortexed before being pelleted in a microfuge. The supernatants from this centrifugation were designated cytosolic extracts.

Each nuclear pellet was resuspended in 50 μl of extraction buffer, consisting of 10 m*M* HEPES, pH 7.9, 400 m*M* NaCl, 10 m*M* KCl, 0.1 m*M* EDTA, 0.1 m*M* EGTA, 1 m*M* DTT, 0.5 m*M* phenylmethylsulfonyl fluoride, and 2 mg/ml of aprotinin, then placed on ice for 30 minutes. The nuclear extracts were pelleted, and the supernatants from this step were designated nuclear extracts.

Oligonucleotide labeling and electrophoretic mobility shift assay (EMSA). The probe consisted of NF-κB–specific double-stranded oligonucleotides with the sequence 5′-AGTTGAGGGGACTTTCCCAGGC-3′ containing the κB site from the κ light chain enhancer in B cells. Oligonucleotides were end-labeled with γ^{32}P-ATP with the use of polynucleotide kinase, and unincorporated γ^{32}P-ATP was removed with Sephadex G-25–packed spin columns (Pharmacia, Uppsala, Sweden).

EMSA was carried out as previously described (27). Briefly, 1 μg of nuclear extract was mixed with the labeled probes in a 20-μl volume in buffer (10 m*M* HEPES, pH 7.9, 50 m*M* KCl, 0.2 m*M* EDTA, 2.5 m*M* DTT, 10% glycerol, and 0.05% Nonidet P-40). The specificity of the complex was analyzed by incubation with an excess of unlabeled competitor oligonucleotides (100-fold molar excess of labeled probe). Samples were run on 7.5% polyacrylamide gels. Next, gels were dried at 80°C for 2 hours then exposed to Kodak X-Omat AR-5 film (Eastman Kodak, Rochester, NY) at −70°C.

Western blot analysis of MMP-9 and IκBα. Secretion of MMP-9 from treated and untreated cells and the contents of IκBα protein in cytosolic extracts obtained from treated and untreated cells were examined by Western blot analysis. Conditioned medium and cytosolic extract containing 20 μg of protein each were subjected to electrophoresis in 15% SDS–polyacrylamide gel electrophoresis, then transferred to a nitrocellulose membrane. The membranes were blocked with 3% bovine serum albumin and incubated with an anti-human MMP-9 antibody (Oncogene Research Products, Cambridge, MA) or with an antibody specific for IκBα (Rockland, Gilbertsville, PA). After intervening rinses with phosphate buffered saline, the antibody was detected using a chemiluminescence Western blotting kit (Amersham, Tokyo, Japan) according to the manufacturer's instructions.

RNA isolation and reverse transcriptase–polymerase chain reaction (RT-PCR). Cells were pretreated for 24 hours with or without cepharanthine (10 μg/ml) and then were treated with either TNFα (10 ng/ml) alone or a combination of TNFα and cepharanthine. Total cellular RNA was isolated at 0 hours and 6 hours after treatment, using the method described by Sambrook et al (28). Complementary DNA was synthesized from 10 μg of total RNA using the Universal RiboClone cDNA Synthesis system (Promega, Madison, WI). The following sense and antisense primers, respectively, were used: for MMP-9, 5′-GGTCCCCCACTGCTGGCCCTTCTACGGCC-3′ and 5′-GCCCACCTCCACTCCTCCCTTTCCTCCAGA-3′ (29); for IκBα, 5′-CGGAATTCCAGGCGGCCGAGCGCCCC-3′ and 5′-GGGGTACCTCATAACGTCAGACGCTG-3′ (27); and for GAPDH, 5′-ACGCATTTGGCTGTATTGGG-3′ and 5′-TGATTTTGGAGGGATCTCGC-3′ (30).

The PCR reactions were conducted in a DNA Thermal Cycler TP-3000 (Takara, Otsu, Japan). After 5 minutes of denaturation at 94°C, 35 cycles of PCR were performed (94°C for 1 minute, 68°C for 1 minute, and 72°C for 1 minute), followed by a final 4-minute extension at 70°C. To visualize the PCR products, the samples were subjected to electrophoresis on a 1% agarose gel, followed by staining with ethidium bromide.

Chloramphenicol acetyltransferase (CAT) assay. The CAT assay was performed using a transient transfection system. A total of 5×10^4 cells were plated in 60-mm plastic petri dishes (Falcon) and pretreated with or without cepharanthine (10 μg/ml) for 24 hours before transfection. Five micrograms of the 5′-flanking region of the MMP-9 gene (54 to −670) linked to the CAT gene as a reporter (−670-CAT) (kindly provided by Dr. Motoharu Seiki, Tokyo University, Tokyo, Japan) was transfected by using a Superfect reagent (Qiagen, Hilden, Germany). At 8 hours after transfection, the culture medium was changed to medium containing either TNFα (10 ng/ml) alone or a combination of TNFα and cepharanthine. Cell lysate was prepared at 12 hours after the change of

medium, and CAT activity was determined with a CAT ELISA kit (Boehringer Mannheim, Mannheim, Germany). The assay was performed at least 3 times.

Morphologic assessment of cepharanthine-pretreated or untreated cells grown on type IV collagen in the presence and absence of TNFα and plasmin. Cells were seeded on 35-mm tissue culture dishes that had been precoated with mouse type IV collagen (Becton Dickinson Labware, Bedford, MA) at a density of 5×10^5/dish. Twenty-four hours after seeding, cells were pretreated with or without cepharanthine (10 μg/ml) for 24 hours. Cells were then treated either with TNFα (50 ng/ml) and plasmin (8 μg/ml; Sigma, St. Louis, MO) (31) or with TNFα, plasmin, and cepharanthine for 96 hours as previously described (16). To monitor morphologic changes, cultures were observed every 24 hours under a phase-contrast microscope (Nikon ELWD 0.3; Nikon, Tokyo, Japan) and photographed with Nikon optics.

RESULTS

Effects of cepharanthine on cell growth. The growth kinetics of NS-SV-AC cells treated with various concentrations of cepharanthine was investigated by MTT assay for up to 4 days. No remarkable cytotoxicity was observed when NS-SV-AC cells were treated with 5 μg/ml or 10 μg/ml of cepharanthine. However, a relatively high dose of cepharanthine (20 μg/ml) significantly inhibited the growth of cells (data not shown). Thus, we selected a concentration of 10 μg/ml for the following experiments.

Effects of cepharanthine on the production of TNFα. Since TNFα stimulates the expression of MMP-9, we examined by ELISA the effect of cepharanthine on the production of TNFα by NS-SV-AC cells. We found that cepharanthine had no effect on the production of TNFα by NS-SV-AC cells (data not shown).

Suppression of MMP-9 activity by cepharanthine. As shown in Figure 1A, clearance of the gelatin substrate at a molecular weight of 92 kd was greatly enhanced in TNFα-treated NS-SV-AC cells (lane 2). However, pretreatment of NS-SV-AC cells with cepharanthine for 24 hours suppressed the activity of TNFα-induced MMP-9 (lane 3).

To further confirm the cepharanthine suppression of TNFα-induced MMP-9 production, conditioned medium was subjected to Western blot analysis. As can be seen in Figure 1B, MMP-9 expression in NS-SV-AC cells was largely augmented by TNFα treatment (lane 2). Consistent with the results of gelatin zymography, cepharanthine pretreatment of the cells prevented the ability of TNFα to stimulate the production of MMP-9 (lane 3). The enzymatic activity and the production of MMP-9 were not detectable at basal levels (lane 1, Figures 1A and B).

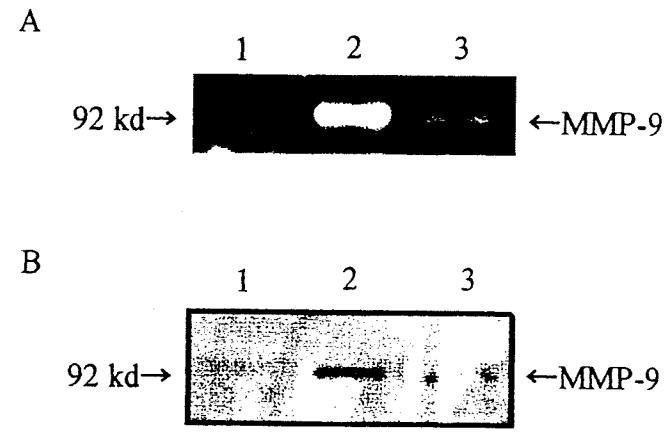

Figure 1. Enzymatic activity of matrix metalloproteinase 9 (MMP-9) and amount of MMP-9 protein in conditioned medium from NS-SV-AC acinar cells treated for 24 hours without (basal level; lane 1) or with tumor necrosis factor α (TNFα; 10 ng/ml) alone (lane 2) or with TNFα plus cepharanthine (10 μg/ml) following a 24-hour pretreatment with cepharanthine (lane 3). **A**, Zymographic analysis revealed that the enzymatic activity of 92-kd MMP-9 was greatly enhanced in TNFα-treated cells compared with untreated cells, whereas pretreatment with cepharanthine followed by TNFα plus cepharanthine led to a drastic reduction of MMP-9 activity. **B**, Similarly, Western blot analysis revealed that although MMP-9 expression was greatly enhanced by TNFα treatment, pretreatment with cepharanthine significantly suppressed the expression of TNFα-induced MMP-9.

Inhibition of MMP-9 mRNA expression and MMP-9 gene promoter activity by cepharanthine. Figure 2 shows the expression of MMP-9 mRNA in NS-SV-AC cells pretreated with or without cepharanthine, followed by treatment for 6 hours with TNFα alone or a combination of cepharanthine and TNFα. The NS-SV-AC cells demonstrated a significant increase in the expression of MMP-9 mRNA (756 bp) in response to TNFα (lane 2). Although MMP-9 mRNA expression was not inhibited by simultaneous treatment with cepharanthine and TNFα (lane 3), cepharanthine pretreatment of the NS-SV-AC cells for 24 hours suppressed the expression of MMP-9 mRNA even after simultaneous treatment with cepharanthine and TNFα (lane 4). Consistent with the results obtained by the analysis at the protein level, MMP-9 mRNA expression was also not detected at the basal level (lane 1).

Thus, RT-PCR analysis confirmed that at the mRNA level, cepharanthine can inhibit TNFα-induced production of MMP-9 protein in NS-SV-AC cells. Equal loading of RNA samples was demonstrated for the

housekeeping gene GAPDH in these RT-PCR experiments.

The 5'-flanking region of the MMP-9 gene (54 to −670) was linked to the CAT gene as a reporter, and cepharanthine suppression of TNFα-induced MMP-9 gene promoter activity was monitored by determining the enzymatic activity expressed in the transiently transfected NS-SV-AC cells. As shown in Figure 3, basal promoter activity (control) was not detected in NS-SV-AC cells. CAT activity was clearly induced in these cells by treatment with TNFα alone as well as with TNFα and cepharanthine, although pretreatment with cepharanthine for 24 hours, followed by simultaneous treatment with TNFα and cepharanthine, resulted in a significant reduction of CAT activity. Thus, it became evident that cepharanthine suppresses the production of MMP-9 protein by inhibiting the TNFα-induced MMP-9 gene promoter activity.

Inhibition of TNFα-induced NF-κB activation by cepharanthine. We previously showed that NS-SV-AC cells constitutively express active NF-κB at the basal level and that p65/p50 heterodimers and p50/p50 homodimers are components of NF-κB (32). In the present study, we examined whether cepharanthine treatment can suppress TNFα-induced NF-κB activity in these cells.

As shown in Figure 4A, when NS-SV-AC cells were treated with TNFα alone, NF-κB DNA binding activity was significantly enhanced, whereas cepharanthine pretreatment followed by treatment with TNFα plus cepharanthine efficiently suppressed the TNFα-induced NF-κB activity (Figure 4B). Accordingly, it became evident that cepharanthine can suppress NF-κB activity induced by TNFα in NS-SV-AC cells. The specific binding of NF-κB to DNA could be abrogated with an excess of unlabeled probe, indicating that this result actually demonstrated the NF-κB activity contained in cells.

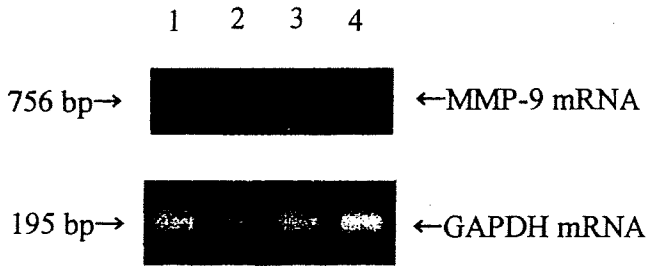

Figure 2. Reverse transcriptase–polymerase chain reaction (RT-PCR) for the expression of matrix metalloproteinase 9 (MMP-9) mRNA in NS-SV-AC acinar cells treated for 6 hours without (basal level; lane 1) or with tumor necrosis factor α (TNFα; 10 ng/ml) alone (lane 2), with a combination of TNFα plus cepharanthine (10 μg/ml) (lane 3), or with a combination of TNFα plus cepharanthine following a 24-hour pretreatment with cepharanthine (lane 4). Treatment with TNFα alone and treatment with TNFα plus cepharanthine significantly induced MMP-9 mRNA expression. However, pretreatment with cepharanthine followed by treatment with TNFα plus cepharanthine almost completely suppressed the expression of MMP-9 mRNA. The mode of MMP-9 mRNA expression (756 bp) was similar to that detected by gelatin zymography and Western blot analysis.

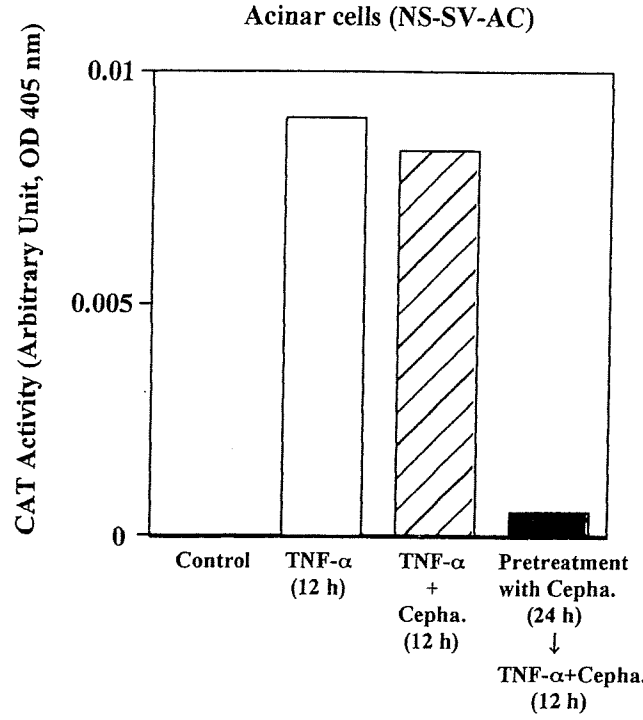

Figure 3. Transcriptional activity of the matrix metalloproteinase 9 (MMP-9) gene promoter in NS-SV-AC acinar cells, as determined by measurement of chloramphenicol acetyltransferase (CAT) activity. The reporter plasmid −670-CAT (5 μg) was transfected into the cells, and the cells were treated for 12 hours without (control) or with tumor necrosis factor α (TNFα; 10 ng/ml) alone, with a combination of TNFα plus cepharanthine (Cepha.; 10 μg/ml), or with a combination of TNFα plus cepharanthine following a 24-hour pretreatment with cepharanthine. No basal promoter activity (control) was detected. Consistent with the results obtained by gelatin zymography, Western blot, and RT-PCR analyses, treatment with TNFα alone or with a combination of TNFα plus cepharanthine significantly augmented CAT activity. However, pretreatment with cepharanthine, followed by treatment with TNFα plus cepharanthine caused a drastic reduction of CAT activity. Results are representative of 3 experiments. OD = optical density.

Partial prevention of TNFα-induced degradation of IκBα protein by cepharanthine. The suppressed NF-κB DNA binding could be due to blocking of IκBα protein or to increased steady-state mRNA levels in

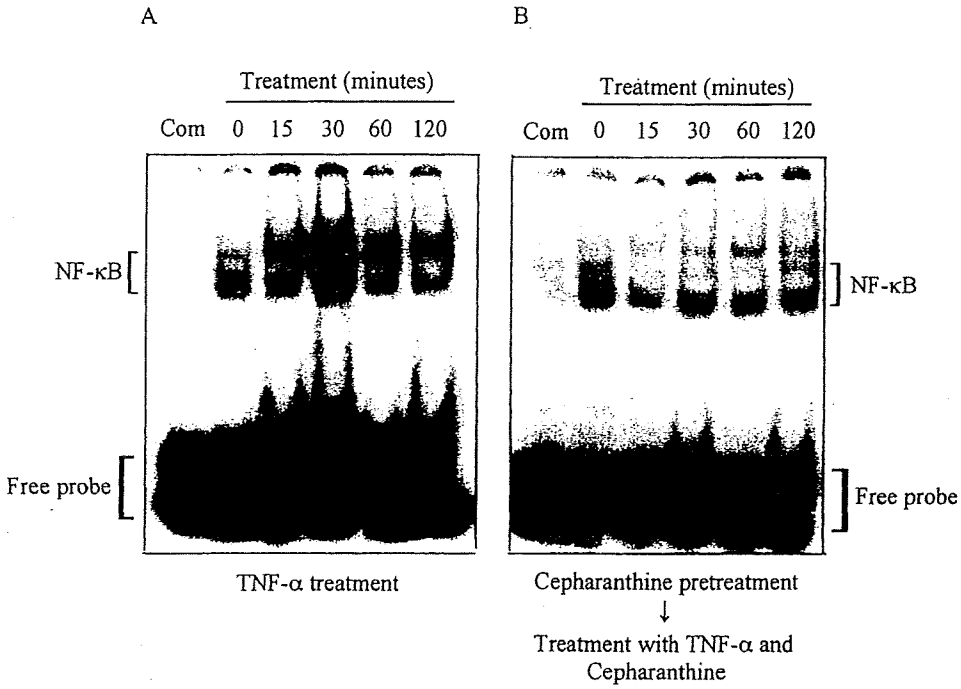

Figure 4. Electrophoretic mobility shift assay analyzing the suppressive effects of cepharanthine (10 μg/ml) on nuclear factor κB (NF-κB) activity in tumor necrosis factor α (TNFα; 10 ng/ml)–treated NS-SV-AC acinar cells. **A,** Cells were treated with TNFα for the indicated times. TNFα treatment caused an enhancement of NF-κB DNA binding activity. **B,** Following a 24-hour pretreatment with cepharanthine, cells were treated with TNFα plus cepharanthine for the indicated times. TNFα plus cepharanthine treatment caused a significant suppression of NF-κB activity, indicating that cepharanthine inhibits TNFα-induced NF-κB activity. The specificity of the complex was analyzed by incubation with a 100-fold excess of unlabeled κB oligonucleotide (Com).

cepharanthine-treated NS-SV-AC cells. To determine which of these two conditions occurred, we examined the expression of IκBα protein and mRNA in cepharanthine-treated cells.

Complete degradation of IκBα protein was observed at 30 minutes after treatment of NS-SV-AC cells with TNFα alone (Figure 5A). After 60 minutes of TNFα treatment, newly synthesized IκBα was detected in cytosols, indicating early NF-κB activation. Thus, IκBα protein underwent a cycle of proteolysis/resynthesis during 60 minutes of TNFα treatment of NS-SV-AC cells. However, cepharanthine pretreatment of NS-SV-AC cells followed by treatment with TNFα plus cepharanthine partially prevented the degradation of IκBα protein (Figure 5B).

RT-PCR analysis, on the other hand, revealed that NS-SV-AC cells did not show any change in the expression of IκBα mRNA in response to cepharanthine pretreatment (Figure 5C). These results therefore suggest that cepharanthine inhibited NF-κB activity in NS-SV-AC cells through partial blocking of the TNFα-induced degradation of IκBα protein.

Morphogenetic profiles of cells grown on type IV collagen. Twenty-four hours after seeding on type IV collagen, NS-SV-AC cells showed the rounded or polygonal-shaped morphology characteristic of the acinar cell phenotype (data not shown) (23). NS-SV-AC cells were cultured for 96 hours with type IV collagen as described in Materials and Methods and examined with phase-contrast microscopy. Following the addition of TNFα (50 ng/ml) and plasmin to the medium, NS-SV-AC cells revealed a loss of tight cell–substrate interactions (Figure 6B) compared with controls (Figure 6A). As shown in our previous study (16), floating cells obtained by treatment with both TNFα and plasmin for 96 hours were confirmed to be apoptotic on examination of Hoechst 33258–stained NS-SV-AC nuclei. In contrast, the in vitro morphogenesis of cepharanthine-

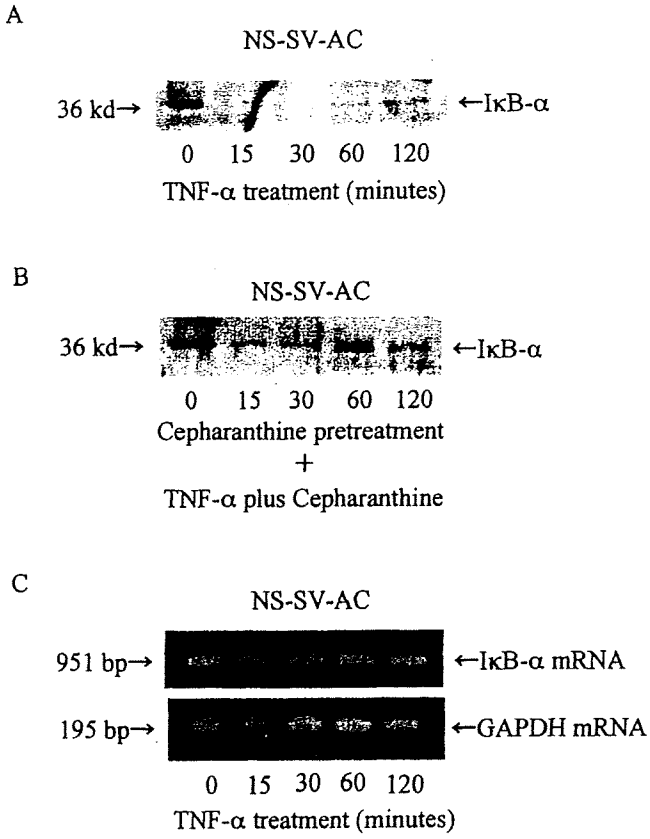

Figure 5. Effects of cepharanthine on the expression of inhibitor of nuclear factor κBα (IκBα) protein and mRNA in NS-SV-AC acinar cells. **A,** Treatment with tumor necrosis factor α (TNFα; 10 ng/ml) resulted in the complete disappearance of IκBα protein at 30 minutes after treatment, as shown by Western blotting. **B,** A 24-hour pretreatment with cepharanthine (10 μg/ml) prior to treatment with TNFα plus cepharanthine resulted in partial prevention of the IκBα protein degradation, as shown by Western blotting. **C,** Pretreatment with cepharanthine for 24 hours prior to treatment with TNFα alone resulted in stable expression of IκBα mRNA (951 bp), as shown by reverse transcriptase–polymerase chain reaction (RT-PCR) analysis of cDNA from the TNFα-treated cells. RT-PCR was performed using sense and antisense primers specific for IκBα and GAPDH.

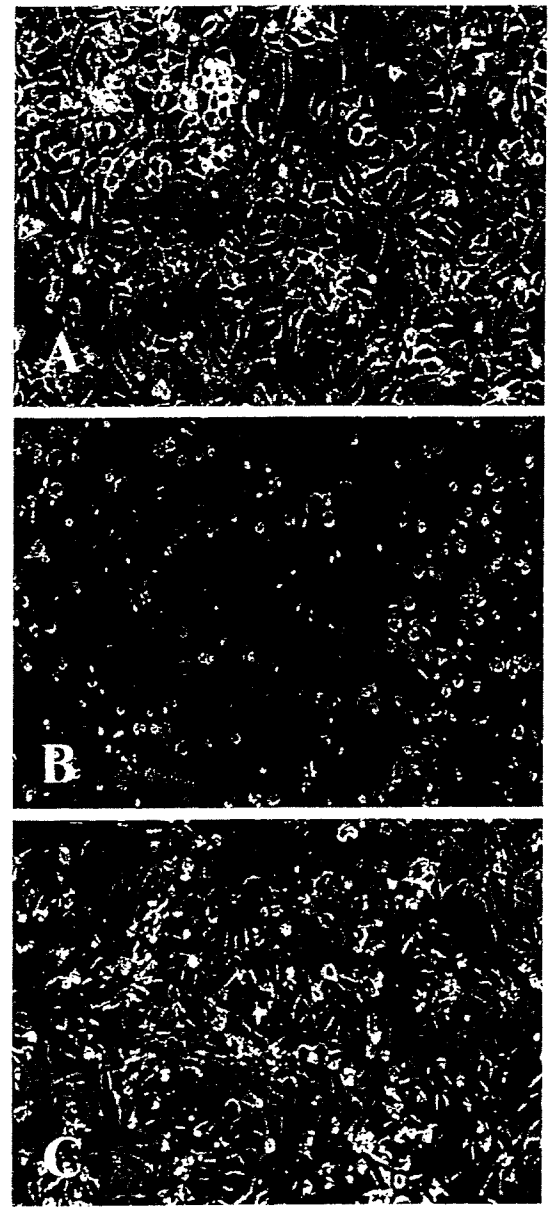

Figure 6. In vitro morphogenetic behavior of NS-SV-AC acinar cells cultured on type IV collagen–coated plates. Cells were cultured for 96 hours in serum-free keratinocyte medium without (control) or with tumor necrosis factor α (TNFα; 50 ng/ml) plus plasmin (8 μg/ml) or with TNFα, plasmin, and cepharanthine (10 μg/ml) following a 24-hour pretreatment with cepharanthine. Plates were then examined by phase-contrast microscopy. **A,** The morphologic appearance of control cells was a round or polygonal shape, with tight attachment to the substrate. **B,** Treatment with TNFα plus plasmin resulted in a loss of tight cell–substrate interactions. **C,** Cepharanthine pretreatment prior to TNFα, plasmin, and cepharanthine treatment resulted in a morphologic appearance similar to that of the control cells. (Original magnification × 100.)

pretreated NS-SV-AC cells was not affected by treatment with the combination of TNFα, plasmin, and cepharanthine, as observed with phase-contrast microscopy (Figure 6C).

DISCUSSION

We have previously shown that the expression of both MMP-9 and p65, one of the components of NF-κB, is up-regulated in SS acinar cells located near infiltrated lymphocytes, where destruction of the acinar structure

seems to occur, compared with both the expression in cells distant from the infiltrated lymphocytes and the expression in cells from normal salivary glands (16). We also found evidence that although acinar (NS-SV-AC) cells entered apoptosis when cultured on type IV collagen–coated dishes in the presence of TNFα and plasmin, suppression of TNFα-induced MMP-9 production by the introduction of srIκBα cDNA corrected the aberrant in vitro morphogenesis of these cells (16). The importance of interactions between the cell and the basement membrane to the survival of cells has also been reported in normal endothelial and prostate cancer cells (33,34). Our previous results therefore indicate that MMP-9 would be one of the causal molecules in the destruction of the acinar structure in the salivary glands of SS patients and that suppression of MMP-9 activity in acinar cells may provide a therapeutic strategy for clinical improvement in SS salivary glands.

In the present study, we found that pretreatment of acinar cells with cepharanthine enables them to survive on the type IV collagen substrate, even after treatment with TNFα and cepharanthine. We selected cepharanthine for our studies of the suppression of TNFα-induced NF-κB activity because cepharanthine has been shown to function as an anti-allergic agent and to reverse the anticancer drug resistance phenotype of cancer cells (19,35,36). The expression of proinflammatory cytokines, such as TNFα, IL-1, IL-6, and IL-8, is positively regulated by NF-κB activity (37,38), and suppression of NF-κB in cancer cells augments sensitivity to anticancer drug–induced apoptosis (39–41). Based on the finding that the MMP-9 gene has a possible binding site for NF-κB in its promoter region (12), we speculated that cepharanthine could inhibit TNFα-induced MMP-9 production by suppressing NF-κB activity in human salivary acinar cells. The findings of our study showed that cepharanthine has the ability to inhibit TNFα-induced MMP-9 production via suppression of TNFα-stimulated NF-κB activity.

Although pretreatment of NS-SV-AC cells with cepharanthine followed by treatment with TNFα plus cepharanthine almost completely inhibited both the transactivation of the MMP-9 gene promoter activity and the production of MMP-9, it seemed likely that the degree of blocking of IκBα degradation by cepharanthine treatment did not necessarily parallel the effects observed in the MMP-9 experiments. We do not currently have a precise explanation for this discrepancy, although Han and Brasier (42) demonstrated that while IκBα appears to be the main regulator of TNFα-induced NF-κB activation in most of the cells, another member of the IαB protein family, IκBβ, also plays a key role in the NF-κB activation by TNFα. This indicates that several IκB proteins, such as IκBα, IκBβ, and IκBε (43), may cooperatively participate in the cepharanthine-mediated prevention of protein degradation.

The novel result among our findings is that cepharanthine suppresses TNFα-induced MMP-9 production through inhibition of NF-κB activity in NS-SV-AC cells. Although we have not yet identified in detail the mechanism involved in the cepharanthine-induced inhibition of NF-κB activity, except to discern that blocking of the degradation of IκBα protein is involved, several possibilities can be suggested. More specifically, a decrease in the activity of IκB kinase or in the ubiquitination or proteasome-mediated degradation of IκBα, IκBβ, or IκBε could explain the cepharanthine-mediated inhibition of TNFα-induced NF-κB activation (44). Further investigation is necessary to clarify the mechanism by which cepharanthine inhibits the TNFα-stimulated degradation of IκB.

An unexpected result from the EMSA study was that although NS-SV-AC cells expressed relatively high levels of NF-κB activity at the basal level, the transcriptional activity of the MMP-9 gene and the expression of MMP-9 protein were extremely low. Although in this study, we did not identify the mechanisms involved in the suppression of MMP-9 expression in NS-SV-AC cells at the basal level, it has recently been shown that transcription of IL-8 and IFNβ genes, both of which are reported to have a κB motif in their promoter regions (45,46), is inhibited at the basal level via binding of NF-κB–repressing factor (NRF) to their negative regulatory element (NRE). That is, under unstimulated conditions, transcription of IL-8 and IFNβ genes is constitutively repressed by NRF in their promoter regions, which partly overlap with the NF-κB response element. Conversely, upon stimulation by external stimuli, by binding to the NRE of the IL-8 and IFNβ promoters, NRF plays an additional role and acts as a coactivator of cytokine-induced IL-8 and IFNβ gene expression (47,48). Thus, since we also have shown that MMP-9 expression is significantly induced by TNFα in NS-SV-AC cells and that NRF has been detected in NS-SV-AC cells (Azuma M et al: unpublished data), it seems likely that NRF may actually function in our in vitro system.

Similar to cepharanthine, the antiinflammatory drugs sodium salicylate and aspirin have been shown to inhibit the activation of NF-κB by preventing the degradation of IκBα protein (49). The effects of salicylate and aspirin on the suppression of NF-κB activity, however,

were observed at suprapharmacologic concentrations (>5 m*M*). In contrast, we have found that cepharanthine is effective at a 2,900-fold lower concentration (10 μg/ml, or ~1.7 μM), which suggests that cepharanthine is a potent inhibitor of MMP-9 activity. Selective gelatinase inhibitors could also suppress TNFα-induced MMP-9 activity (50) and may prove useful for the prevention of the destruction of acinar structure. However, in addition to the suppressive effect on TNFα-induced MMP-9 production, cepharanthine has the ability to inhibit the secretion of TNFα from infiltrated lymphocytes (51). Cepharanthine would therefore be effective in terms of both inhibiting the release of TNFα from lymphocytes and suppressing the TNFα-induced MMP-9 production. Furthermore, it is recognized that cepharanthine is a safe agent even if administered for a long period of time, and it is used widely in Japan.

Our results suggest that cepharanthine would be a promising agent for use in the treatment of salivary gland involvement in patients with SS. It may also have applications in various other diseases in which NF-κB activation has been shown to mediate pathogenesis, including arthritis and oral lichen planus. These possibilities warrant further investigation.

REFERENCES

1. Alspaugh MA, Whaley WW, Wohl MJ, Bunin JJ. Sjögren's syndrome. In: Kelley WN, Harris ED Jr, Ruddy S, Sledge CB, editors. Textbook of rheumatology. Philadelphia: WB Saunders; 1981. p. 971–99.
2. Daniel TE. Labial salivary gland biopsy in Sjögren's syndrome: assessment as a diagnostic criterion in 362 suspected cases. Arthritis Rheum 1984;27:147–56.
3. Hamano H, Saito I, Haneji N, Mitsuhashi Y, Miyasaka N, Hayashi Y. Expression of cytokine genes during development of autoimmune sialadenitis in MRL/lpr mice. Eur J Immunol 1993;23: 2387–91.
4. Fox RI, Kang H-I, Ando D, Abrams J, Pisa E. Cytokine mRNA expression in salivary gland biopsies of Sjögren's syndrome. J Immunol 1994;152:5532–9.
5. Bernfield M, Banerjee SD, Cohn RH. Dependence of salivary epithelial morphology and branching morphogenesis upon acid mucopolysaccharide protein (proteoglycan) at the epithelial surface. J Cell Biol 1972;52:674–89.
6. Dayer J-M, Beutler B, Cerami A. Cachectin/tumor necrosis factor stimulates collagenase and prostaglandin E_2 production by synovial cells and dermal fibroblasts. J Exp Med 1985;162:2163–8.
7. Goldring MB, Birkhead JR, Suen L-F, Yamin R, Mizuno S, Glowacki J, et al. Interleukin-1β-modulated gene expression in immortalized human chondrocytes. J Clin Invest 1994;94:2307–16.
8. Konttinen YT, Kangaspunta P, Lindy O, Takagi M, Sorsa T, Segerberg M, et al. Collagenase in Sjögren's syndrome. Ann Rheum Dis 1994;53:836–9.
9. Hanemaaijer R, Visser H, Konttinen YT, Koolwijk P, Verheijen JH. A novel and simple immunocapture assay for determination of gelatinase-B (MMP-9) activities in biological fluids: saliva from patients with Sjögren's syndrome contains increased latent and active gelatinase-B levels. Matrix Biol 1998;17:657–65.
10. Konttinen YT, Halinen S, Hanemaaijer R, Sorsa T, Hietanen J Ceponis A, et al. Matrix metalloproteinase (MMP)-9 type IV collagenase/gelatinase implicated in the pathogenesis of Sjögren's syndrome. Matrix Biol 1998;17:335–47.
11. Simon C, Goepfert H, Boyd D. Inhibition of the p38 mitogen activated protein kinase by SB 203580 blocks PMA-induced M 92,000 type IV collagenase secretion and in vitro invasion. Cancer Res 1998;58:1135–9.
12. Sato H, Seiki M. Regulatory mechanism of 92 kDa type IV collagenase gene expression, which is associated with invasiveness of tumor cells. Oncogene 1993;8:395–405.
13. Okada Y, Tsuchiya H, Shimizu H, Tomita K, Nakanishi I, Sato H, et al. Induction and stimulation of 92-kDa gelatinase/type IV collagenase production in osteosarcoma and fibrosarcoma cell lines by tumor necrosis factor α. Biochem Biophys Res Commun 1990;171:610–7.
14. Beg AA, Ruben SM, Scheinman RI, Haskill S, Rosen CA, Baldwin AS Jr. IκB interacts with the nuclear localization sequences of the subunits of NF-κB: a mechanism for cytoplasmic retention. Genes Dev 1992;6:1899–913.
15. Karin M. The beginning of the end: IκB kinase (IKK) and NF-κB activation. J Biol Chem 1999;274:27339–42.
16. Azuma M, Aota K, Tamatani T, Motegi K, Yamashita T, Harada K, et al. Suppression of tumor necrosis factor α–induced matrix metalloproteinase 9 production by the introduction of a super-repressor form of inhibitor of nuclear factor κBα complementary DNA into immortalized human salivary gland acinar cells: prevention of the destruction of the acinar structure in Sjögren's syndrome salivary glands. Arthritis Rheum 2000;43:1756–67.
17. Azuma M, Motegi K, Aota K, Hayashi Y, Sato M. Role of cytokines in the destruction of acinar structure in Sjögren's syndrome salivary glands. Lab Invest 1997;77:269–80.
18. Gutterman JU, Fien S, Quesada J, Horning SJ, Levine JF, Alexanian R, et al. Recombinant leukocyte A interferon: pharmacokinetics, single-dose tolerance, and biologic effects in cancer patients. Ann Intern Med 1982;96:549–56.
19. Hamburger AW, Salmon SE. Primary bioassay of human tumor stem cells. Science 1977;197:461–3.
20. Havell EA, Vilcek J. Inhibition of interferon secretion by vinblastine. J Cell Biol 1975;64:716–9.
21. Ono M. Antitumor effect of cepharanthin: activation of regional lymph node lymphocytes by intratumoral administration. Clin Immunol 1987;19:1061–4.
22. Morioka S, Ono M, Tanaka N, Orita K. Synergistic activation of rat alveolar macrophages by cepharanthin and OK-432. Jpn J Cancer Chemother 1985;12:1470–5.
23. Azuma M, Tamatani T, Kasai Y, Sato M. Immortalization of normal human salivary gland cells with duct-, myoepithelial-, acinar-, or squamous phenotype by transfection of SV40 ori-mutant DNA. Lab Invest 1993;69:24–42.
24. Azuma M, Tamatani T, Fukui K, Bando T, Sato M. Enhanced proteolytic activity is responsible for the aberrant morphogenetic development of SV40-immortalized normal human salivary gland cells grown on basement membrane components. Lab Invest 1994;70:217–27.
25. Herron GS, Banba MJ, Clark EJ, Gavrilovic J, Werb Z. Secretion of metalloproteinases by stimulated capillary endothelial cells. J Biol Chem 1986;261:2814–8.
26. Claudio E, Segada F, Wrobel K, Ramos S, Bravo R, Lazo PS. Molecular mechanism of TNFα cytotoxicity: activation of NF-κB and nuclear translocation. Exp Cell Res 1996;224:63–71.
27. Imbert V, Rupec RA, Livolsi IA, Pahl HL, Traenckner EB-M, Mueller-Dieckmann C, et al. Tyrosine phosphorylation of IκBα activates NF-κB without proteolytic degradation of IκBα. Cell 1996;86:787–8.

28. Sambrook J, Fritsch EF, Maniatis T. Extraction, purification, and analysis of messenger RNA from eukaryotic cells. In: Molecular cloning, a laboratory manual. 2nd ed. New York: Cold Spring Harbor Laboratory Press; 1989. p. 7.01–7.83.
29. Liabakk N-B, Talbot I, Smith RA, Wilkinson K, Balkwill F. Matrix metalloproteinase 2 (MMP-2) and matrix metalloproteinase 9 (MMP-9) type IV collagenases in colorectal cancer. Cancer Res 1996;56:190–6.
30. Yamaguchi F, Saya H, Bruner JM, Morrison RS. Differential expression of two fibroblast growth factor-receptor genes is associated with malignant progression in human astrocytomas. Proc Natl Acad Sci U S A 1994;91:484–8.
31. Agrez M, Gu X, Turton J, Meldrum C, Niu J, Antalis T, et al. The $\alpha v\beta 6$ integrin induces gelatinase B secretion in colon cancer cells. Int J Cancer 1999;81:90–7.
32. Azuma M, Motegi K, Aota K, Yamashita T, Yoshida H, Sato M. TGF-β1 inhibits NF-κB activity through induction of IκB-α expression in human salivary gland cells: a possible mechanism of growth suppression by TGF-β1. Exp Cell Res 1999;250:213–22.
33. Aoudjit F, Vuori K. Matrix attachment regulates Fas-induced apoptosis in endothelial cells: a role for c-Flip and implication for anoikis. J Cell Biol 2001;152:633–43.
34. Jiang C, Wang Z, Ganther H, Lu J. Caspases as key executors of methyl selenium-induced apoptosis (anoikis) of DU-145 prostate cancer cells. Cancer Res 2001;61:3062–70.
35. Hotta T, Tanimura H, Yamaue H, Iwahashi M, Tani M, Tsunoda T, et al. Synergistic effects of tamoxifen and cepharanthine for circumventing multidrug resistance. Cancer Lett 1996;107:117–23.
36. Asaumi J, Nishikawa K, Matsuoka H, Iwata M, Kawasaki S, Hiraki Y, et al. Direct antitumor effect of cepharanthin and combined effect with adriamycin against Ehrlich ascites tumor in mice. Anticancer Res 1995;15:67–70.
37. Duffey DC, Chen Z, Dong G, Ondrey FG, Wolf JS, Brown K, et al. Expression of a dominant-negative mutant inhibitor-κBα of nuclear factor-κB in human head and neck squamous cell carcinoma inhibits survival, proinflammatory cytokine expression, and tumor growth in vivo. Cancer Res 1999;59:3468–74.
38. Dong G, Chen Z, Kato T, Wuges CV. The host environment promotes the constitutive activation of nuclear factor κB and proinflammatory cytokine expression during metastatic tumor progression of murine squamous cell carcinoma. Cancer Res 1999;59:3495–504.
39. Beg AA, Baltimore D. An essential role for NF-κB in preventing TNF-α induced cell death. Science 1996;274:782–4.
40. Wang C-Y, Mayo MW, Baldwin AS Jr. TNF- and cancer therapy-induced apoptosis: potentiation by inhibition of NF-κB. Science 1996;274:784–7.
41. Van Antwerp DJ, Marin SJ, Kafri T, Green DR, Verma IM. Suppression of TNF-α-induced apoptosis by NF-κB. Science 1996; 274:787–9.
42. Han Y, Brasier AR. Mechanism for biphasic Rel A: NF-κB1 nuclear translocation in tumor necrosis factor α-stimulated hepatocytes. J Biol Chem 1997;272:9825–32.
43. Baldwin AS Jr. The NF-κB and IκB proteins: new discoveries and insights. Annu Rev Immunol 1996;14:649–83.
44. Yamamoto Y, Yin M-J, Lin K-M, Gaynor RB. Sulindac inhibits activation of the NF-κB pathway. J Biol Chem 1999;274:27307–14.
45. Mukaido N, Morita M, Ishikawa Y, Rice N, Okamoto SI, Kasahara T, et al. Novel mechanism of glucocorticoid mediated gene repression: nuclear factor κB is target for glucocorticoid mediated interleukin-8 gene repression. J Biol Chem 1994;269:13289–95.
46. Thanos D, Maniatis T. Identification of the rel family members required for virus induction of the human β interferon gene. Mol Cell Biol 1995;15:152–64.
47. Nourbakhsh M, Kälble S, Dörrie A, Hauser H, Resch K, Kracht M. The NF-κB repressing factor is involved in basal repression and interleukin (IL)-1-induced activation of IL-8 transcription by binding to a conserved NF-κB-flanking sequence element. J Biol Chem 2001;276:4501–8.
48. Nourbakhsh M, Hauser H. Constitutive silencing of IFN-β promoter is mediated by NRF (NF-κB-repressing factor), a nuclear inhibitor of NF-κB. EMBO J 1999;18:6415–25.
49. Kopp E, Ghosh S. Inhibition of NF-κB by sodium salicylate and aspirin. Science 1994;265:956–9.
50. Koivunen E, Arap W, Valtanen H, Rainisalo A, Medina OP, Heikkila P, et al. Tumor targeting with a selective gelatinase inhibitor. Nat Biotechnol 1999;17:768–74.
51. Ono M, Tanaka N, Tsuji M. Anti-inflammatory action of cepharanthin ointment ingredient in experimental animals: studies for the chronic inflammation and TNF-α production. Jpn J Inflamm 1994;14:425–9.

Exp. Anim. 53(2), 171–173, 2004

—Note—

Differences in Responsiveness of Mouse Strain against p-Benzoquinone as Assessed by Non-Radioisotopic Murine Local Lymph Node Assay

Masahiro TAKEYOSHI, Shuji NODA, and Kanji YAMASAKI

Hita Laboratory, Chemicals Evaluation and Research Institute, Japan, 3–822, Ishii-machi, Hita-shi, Oita 877-0061, Japan

Abstract: *The non-radioisotopic modification of murine local lymph node assay (LLNA) by using 5-bromo-2'-deoxyuridine (BrdU) was conducted to investigate the strain-related difference of the responsiveness of mice to* p*-benzoquinone (PBQ) with BALB/cAnN, CBA/JN and CD-1 mouse strains. Strain and dose related differences were analyzed by two-way analysis of variance (two-way ANOVA). CBA/JN was considered to be the highest responsive strain to PBQ, and interaction was detected between CD-1 and each of the other inbred strains. These results support the recommendation in the OECD test guideline 429 and the skin sensitization test guideline of US-EPA with regard to the selection of mouse strain for LLNA.*

Key words: *local lymph node assay, responsiveness,* p*-benzoquinone*

Contact dermatitis caused by chemicals is a serious health problem, and a prediction of the skin sensitizing potential of chemicals is necessary to secure safe handling of chemicals. The guinea pig maximization test and the Buehler test have been widely used for predicting the skin sensitizing potentials of chemicals for regulatory purposes for a long time [1, 6]. Recently the murine local lymph node assay (LLNA) has been recognized as a new stand-alone sensitization test which can be used for regulatory purposes [3–5], and it is based upon consideration of the induced proliferative responses in lymph nodes draining the site of topical exposure to the test chemical. In the standard LLNA, cell proliferation is measured using the incorporation of radiolabeled thymidine or uridine into draining lymph node cells, and this requires specific facilities and handling conditions. We previously developed a non-radioisotopic alternative method for the LLNA which uses 5-bromo-2'-deoxyuridine (BrdU) incorporation in place of radioisotopes [9, 10]. The responsiveness of mouse strains against antigen is known to vary with their H-2 haplotypes. We report here the difference of responsiveness of three mouse strains in the modified murine local lymph node assay against *p*-benzoquinone, a known potent contact allergen to human.

p-Bebzoquinone (BZQ, Lot No. 012D2294, Kanto Chemical Co., Tokyo, Japan) was dissolved in acetone:olive oil (AOO; 4:1). 5-Bromo-2'-deoxyuridine (BrdU, Nacalai Tesque, Kyoto, Japan) was dissolved in

(Received 22 September 2003 / Accepted 25 December 2003)

Address corresponding: M. Takeyoshi, Hita Laboratory, Chemicals Evaluation and Research Institute, Japan, 3–822, Ishii-machi, Hita-shi, Oita 877-0061, Japan